Marine Environmental Science

MASTER THESIS

Daily patterns of clock gene expression in Antarctic krill, *Euphausia superba*, under a 12h:12h light:dark cycle in the laboratory

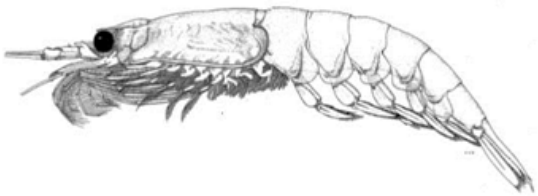

SUBMITTED BY: Lisa Pitzschler

PRINCIPAL SUPERVISOR: Prof. Dr. Bettina Meyer

Co-SUPERVISOR: Dr. Stefanie Moorthi

March 7, 2018

MASTER THESIS

Daily patterns of clock gene expression in Antarctic krill,
Euphausia superba, under a 12h:12h light:dark cycle in the laboratory
Submitted: March 7, 2018

SUBMITTED BY

Lisa Pitzschler
M. Sc. Marine Environmental Science
Carl von Ossietzky University of Oldenburg
Carl-von-Ossietzky-Straße 9-11, 26111 Oldenburg

PRINCIPAL SUPERVISOR

Prof. Dr. Bettina Meyer
Institute for Chemistry and Biology of the Marine Environment (ICBM)
Section: Biodiversity and biological processes in polar oceans
Carl-von-Ossietzky-Straße 9-11, 26111 Oldenburg

Alfred-Wegener -Institute
Helmholtz Centre for Polar- and Marine Research
Section: Polar biological oceanography
Am Handelshafen 12, 27570 Bremerhaven

Co-SUPERVISOR

Dr. Stefanie Moorthi
Institute for Chemistry and Biology of the Marine Environment (ICBM)
Section: Planktology
Schleusenstraße 1, 26382 Wilhelmshaven

Abstract

The Southern Ocean is a region with strong seasonality in sea ice coverage, food supply and photoperiod (the day length). Antarctic krill (*Euphausia superba*) a key organism in this habitat show remarkable adaptation to this environment by evolving daily and seasonal rhythmicity of physiological and behavioural functions. Recent investigations of these rhythms have demonstrated that an endogenous circadian clock times metabolic output rhythms in krill, synchronized by photoperiod. In krill, the mechanisms of clock genes and their products, however, leading to these rhythms, the distributions of the genes as well as chronobiological functions are essentially unknown. The present study aims for a more comprehensive analysis of endogenous circadian regulation in Antarctic krill, especially with regard to possible optimization of the methodological approach to the identification of putative rhythmic gene expression patterns in brain and eyestalks of krill, in the laboratory. Within this study, were able to demonstrate significant 24h rhythmic oscillation for *Cyc* and *Vri* in brain and in general within the eyestalks more pronounced patterns and agreement with literature, could be identified. We further conclude that gene expression probably play the same role in both tissues, except for *Dbt*. However, we conclude that the analysis of the whole head is more suitable for the future, because amplitudes of the oscillation are the same and only *Dbt* obtained differences in gene expression within the tissues. Moreover, there is probably first evidence that the interactions between the genes within a tissue might be displaced by a 4 hour rhythm as well as that the transmission between the tissues needs a larger time frame. Further studies in Antarctic krill needs to investigate more knowledge on chronobiological behavior and the associated endogenous timing system, on the contributions of individual clock genes on transcriptional as well as on protein level and on neuroanatomical signal perception and transmission.

Key words: Antarctic krill, circadian clock, clock genes, brain and eyestalks, laboratory, relative mRNA level, 12L:12D

Zusammenfassung

Das Südpolarmeer ist eine Region mit ausgeprägter Saisonalität in Hinblick auf Eisbedeckung, Nahrungsmittelversorgung und die Photoperiode (Tageslänge). Antarktischer Krill (*Euphausia superba*), ein Schlüsselorganismus innerhalb dieses Habitats, weist eine bemerkenswerte Anpassung in diesem Umfeld auf, indem er seine tägliche sowie saisonale Rhythmik der Physiologischen,- und Verhaltensfunktion verändert. Neuste Untersuchungen dieser Rhythmen haben bewiesen, dass eine endogene innere Uhr, synchronisiert durch die Photoperiode, den Metabolismus in Krill steuert. Im Krill sind jedoch die Mechanismen von Uhr-Genen und deren Produkten, die zu diesen Rhythmen führen, die Verteilungen der Gene sowie chronobiologische Funktionen im Wesentlichen unbekannt. Die vorliegende Studie zielt auf eine umfassendere Analyse der endogenen zirkadianen Regulation im antarktischen Krill ab, insbesondere in Hinblick auf eine mögliche Optimierung des methodischen Ansatzes, zur Identifizierung von mutmaßlichen rhythmischen Genexpressionsmustern im Gehirn und den Augenstielen von Krill im Labor. Innerhalb dieser Studie konnten signifikante 24h rhythmische Oszillationen für *Cyc* und *Vri* im Gehirn sowie in den Augenstielen identifiziert werden. Zudem konnte gezeigt werden, dass innerhalb der Augenstiele die Genexpressionsmuster deutlich ausgeprägter sind und mit vorhandener Literatur größere Übereinstimmung zeigen. Weiterhin schlussfolgern wir, dass die Genexpression wahrscheinlich die gleiche Rolle in beiden Geweben spielt, mit Ausnahme von *Dbt.* Jedoch können wir auch das Fazit ziehen, dass für zukünftige Experimente die Verwendung des ganzes Kopfes eine bessere Eignung zeigt, da die Amplituden der Oszillation gleich sind und lediglich *Dbt* einen Unterschied zwischen den untersuchten Geweben aufweist. Darüber hinaus gibt es wahrscheinlich erste Hinweise darauf, dass die Interaktionen zwischen den Genen innerhalb eines Gewebes um einen 4-Stunden-Rhythmus verschoben sein könnten, und das Interaktionen zwischen den Geweben einen größeren Zeitrahmen benötigen. Zukünftige Studien im antarktischen Krill sollten darauf abzielen, mehr Wissen über das chronobiologische Verhalten und das damit verbundene endogene Timing-System, über die Beiträge einzelner Uhr-Gene auf Transkriptions- und Proteinebene sowie über die neuroanatomische Signalwahrnehmung und –Übertragung, zu erlangen.

Schlüsselwörter: Antarktischer Krill, innere Uhr, Uhr-Gene, Gehirn und Augenstiele, Labor, relative mRNA Level, 12L:12D

Index

List of figures

List of tables

List of Abbreviations

AK	aldo-keto reductase
cry2 (CRY2)	*chryptochrom 2 (CHRYPTOCHROM 2)*
CS	citrate synthase
Ct	cycle threshold
cwo (CWO)	*clockwork orange (CLOCKWORK ORANGE)*
cyc (CYC)	*cycle (CYCLE)*
dbt2 (DBT2)	*doubletime 2 (DOUBLETIME 2)*
DD	dark:dark (24h darkness)
DVM	diel vertical migration
E	eye
E75	ecdysone induced protein 75
ES	eyestalks
HR3	nuclear hormone receptor 3
LD	light:dark (12h light: 12h dark)
NAGase	N-acetylglucosaminidase
NCBI	National Center for Biotechnology Information
NT	no template
per (PER)	*period (PERIOD)*
RNA	ribonucleic acid
RT	room temperature
+RT	with reverse transcriptase
-RT	without reverse transcriptase
qPCR	real-time quantitative polymerase chain reaction
sgg (SGG)	*shaggy (SHAGGY)*
SO	Southern Ocean
SW	southwest
tim (TIM)	*timeless (TIMELESS)*
TRY	trypsin
Usp46 (USP46)	*ubiquitin specific peptidase 46*
vri (VRI)	*vrille (VRILLE)*

1 Introduction

Antarctic krill (*Euphausia superba;* referred to as krill in the following) is a small euphausiid crustacean with is endemic in the Southern Ocean (SO) (Meyer et al. 2010; Siegel 2016). Over 70 % of its total stock are located in the Atlantic sector of the SO between longitudes 0° and 90°W (Scotia Sea and southern Drake Passage) (Atkinson et al. 2008; Atkinson et al. 2004; Hill et al. 2013). Krill, which their biomass between 67 to 297 million tons, is a key organism in the SO and serves as direct link between primary producers and top predators such as penguins, seals and whales as well as several fish species and also constitute the main fisheries target in this region (Zane et al. 1998; Siegel 2005; Siegel 2016; Asoc 2010).

Changing environmental conditions due to global warming cause an increase in deep ocean temperature as well as a decrease in winter sea-ice duration at several locations (Clarke & Harris 2003; Curran et al. 2003). A positive correlation between krill density and the sea-ice cover suggest that the extent as well as the duration of the sea ice might be fundamental for krill (Atkinson et al. 2004). A strong krill density decline has been observed in concert with the winter sea ice extent and duration since the 1970s in the SW Atlantic sector of the SO (Atkinson et al. 2008; Atkinson et al. 2004). Other studies demonstrated, that also ocean acidification, may impact krill recruitment and population density (Kawaguchi et al. 2013).

Therefore, climate change in addition to an increasing krill fishery (Kawaguchi et al. 2013; Nicol & Yoshinari 1997) may enhance the pressure on krill populations in the future, which profound consequences for the SO food web (Atkinson et al. 2004; Schiermeier 2010). For this reason, it is crucial to understand the machinery of krill's life cycle to make predictions how krill might cope with a changing environment.

1.1 Seasonal and diel rhythms in the life cycle of Antarctic krill (*E. superba*)

The SO is a region with strong seasonal and daily fluctuations in several parameters, such as photoperiod, light intensity, food supply and sea-ice extent (Quetin & Ross 1991). Krill show remarkable adaptation to this environment (Miller, D. G. M. & Hampton 1989) and have evolved seasonal and daily rhythmicity of physiological and behavioral functions (Quetin & Ross 1991; Murphy et al. 2007; Teschke et al. 2011).

1.1.1 Seasonal rhythms

When food is scarce during winter due to sea-ice cover and lack of light, seasonal adaptation of physiological processes could be observed (Quetin & Ross 1991). To cope with the scarcity of food, physiological parameters like oxygen consumption, feeding rates, and metabolic enzyme activity revealed a significant decrease during autumn and winter. For example, Meyer et al. (2010) demonstrated that krill from the field showed reduced respiration rates (30 % to 50 %) as well as reduced feeding activity (80%) in autumn and winter compared to late spring. On the enzyme level, citrate synthase (CS) and MDH (malate dehydrogenase), key enzymes of metabolic activity were also significant reduced compared to summer data, suggesting an energy saving mechanism in krill during periods of low food availability (Teschke et al. 2011; Meyer et al. 2002; Meyer et al. 2010).

Growth is a matter of food supply and temperature and reflected the same patterns, with highest values in spring compared to growth activities in winter (Meyer et al. 2010). In addition, for their utilization during winter when food supply is scarce, krill accumulate large amount of body lipids during summer when high phytoplankton blooms are formed (Meyer et al. 2010). In the laboratory, it has been shown that feeding activity, oxygen consumption and metabolic enzyme activity of MDH in krill are strongly influenced by seasonal changes of photoperiod (Teschke et al. 2007). Parameters increased in krill exposed to constant light (LL) and 12h light and 12h dark conditions (L:D 12:12) whereas, krill exposed to constant darkness (DD) showed no response to the high food availability and also oxygen consumption and metabolic enzyme activity was significantly lower compared to LL and LD light conditions (Teschke et al. 2007).

Also the sexual organs of krill follow a seasonal cycle, with a reduction from autumn to winter and a re-maturation during the up-coming spring (Siegel et al. 2004). The maturity cycle could also be observed in the laboratory, suggesting that the pattern of the cycle as well as the length for completing it seems to be influenced by environmental parameters (food availability, temperature and photoperiod) (Thomas & Ikeda 1987; Kawaguchi et al. 2007). Controlled laboratory studies showed that the photoperiod is essential for the stimulation and induction of maturation and spawning of krill (Hirano et al. 2003; Teschke et al. 2008; Brown et al. 2011).

1.1.2 Daily rhythms

In addition to seasonal cycles, krill perform daily rhythms of migration in the water column to minimize predator risk. They hide in deeper water layers during the day and migrate up to the photic zone during night (Gliwicz 1986). This clear pattern governed by the day-night rhythm can be observed in winter (February to October) whereas DVM is changing in late spring to early summer and accordingly DVM is ceased during summer (October to November) (Cisewski et al. 2010). Diurnal and seasonal fluctuations in DVM and krill swarm aggregation in spring and summer seem to be closely linked to the feeding and spawning ecology of krill (Taki et al. 2005).

In the field, the DVM patterns showed a main 24 h rhythm (night up, day down) as well as a subordinated 12 h rhythm (migrating again during the day), with high food availability this rhythm is ceased and even more pronounced when food is scarce (Godlewska M. 1996; Gaten et al. 2008). Gaten et al. (2008) identified an endogenous rhythm of locomotor activity of specimens under laboratory settings with a period of 12 h and 24 h, which correlate with the findings in the field. Also metabolic key processes such as oxygen consumption and the temporal activity profiles of aerobic key enzyme CS oscillated in an daily 9-12 hour rhythm (Teschke et al. 2011). De Pitta et al. (2013) provided the first insight into the regulation of physiological processes of krill during the Antarctic summer and observed rhythmicity in transcript expression of important processes such as translation, proteolysis, energy and metabolic processes, redox regulation, visual transduction and stress response, which can be related to daily environmental changes.

Therefore, it seems that the regulation of seasonal and daily rhythms in krill physiological processes may be under the control of endogenous mechanisms, which might be influenced by photoperiod.

1.2 Biological clocks control the daily life of organisms

Due to the formation of seasons, tides and the diurnal light cycle, periodic fluctuations determine the life of pretty much every organism on earth (Strauss & Dircksen 2010; Dunlap 1999). As a consequence organisms adapted to these cyclic changes of their environment by evolving periodic fluctuations of physiological and behavioral processes (Roenneberg & Merrow 2005; Teschke et al. 2011). As a cause of evolutionary development light-sensitive organisms, including plants, animals and photosynthesizing cyanobacteria evolved endogenous biological clocks, to adapt diel fluctuations of the environment (Strauss & Dircksen 2010; Roenneberg & Merrow 2005; Dunlap 1999).

1.2.1 Molecular mechanisms of the circadian clock

The molecular mechanisms underlying the eukaryotic circadian clock have first been identified in the fruit fly *Drosophila.* It is based on positive and negative transcriptional and translational feedback loops regulated by a set of clock genes (Dunlap 1999; Roenneberg & Merrow 2005). The circadian system of the fruit fly is very advanced: One of the core oscillatory loops is based on the interaction of the products of *Clock (Clk)* and *cycle (cyc)* genes. By forming a heterodimer they activate the transcription of *period (per)* and *timeless (tim)* during late day to early night (***Fehler! Verweisquelle konnte nicht gefunden werden.***) (Tomioka & Matsumoto 2015). To produce an auto-regulative negative feedback loop, PER and TIM form a heterodimer in the middle of the night, enter the nucleus and suppress their own transcription by inactivating the transcription of Clk/cyc. Moreover, the CLK/CYC heterodimer also activates the transcription of *vrille (vri)* and *Par domain protein 1ε (Pdp1ε)*. Due to the accumulation of the VRI protein, the transcription of *Clk* is suppressed through a V/P box in the *Clk* regulatory region. PDP1ε accumulates later than VRI and paves the way for the *Clk* transcription and consequently, CLK accumulation during the day. The transcription of *clockwork orange (cwo),* regulating the amplitude of *per* and *tim* mRNA oscillation, is also activated by CLK/CYC. The *Drosophila* type *cryptochrome (d-cry or cry1),* which has been identified as the blue light photoreceptor, is known to entrain endogenous clocks due to promoting the light-dependent degradation of TIM (Breedlove 2000; Tomioka & Matsumoto 2015). The mammalian type *chryptochrome* (m-cry or cry2) has lost the ability of photoreception (Tomioka & Matsumoto 2015).

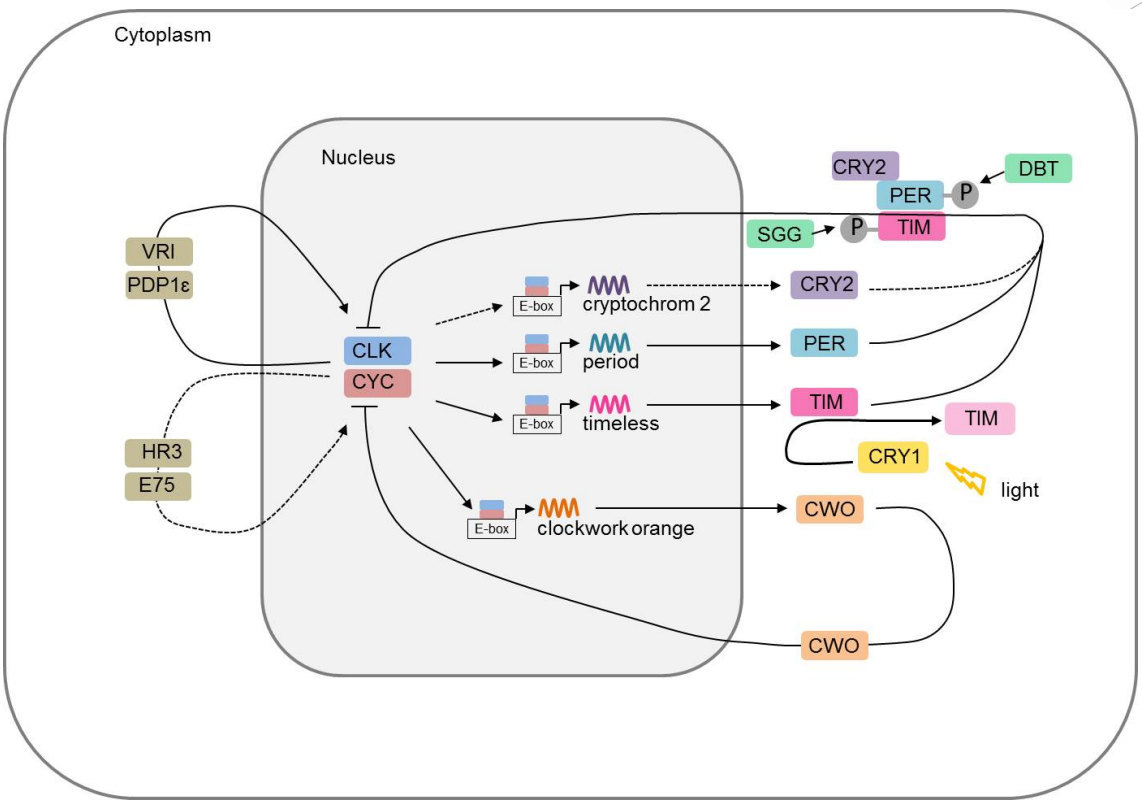

Figure 1: Hypothetical molecular mechanism of the insect circadian clockwork in *Drosophila*. Auto regulative negative feedback loop consists of the transcription factors CLOCK (CLK), CYCLE (CYC), PERIOD (PER) and TIMELESS (TIM). In many insects CRYPTOCHROME2 (CRY2) is known to function as a negative regulator. TIM is degraded by CRY1 in a light-dependent manner to reset the clock's phase. TIM and PER are phosphorylated regulating the timing of nuclear entry by SHAGGY (SGG) and DOUBLETIME (DBT). CLK and CYC are expressed by VRILEE (VRI) and PAR DOMAIN PROTEIN 1ε (PDP1ε) and probably, by HR3 and E75. CLOCKWORK ORANGE (CWO) is regulated by another loop. Solid lines indicate pathways known for *Drosophila*; dashed lines indicate hypothesized clockwork mechanisms in other insects [Adapted from (Tomioka & Matsumoto 2015)].

1.2.2 The circadian clock

Circadian (latin: circa=about, dies= a day) rhythms oscillate within an approximate 24 h rhythm under constant conditions (Kuhlman et al. 2007; Strauss & Dircksen 2010). Endogenous rhythmicity persists even if no entraining by environmental cues occurs (free-running) (Roenneberg & Merrow 2005; Strauss & Dircksen 2010). Therefore, a control by internal pacemakers takes place, which autonomously regulate cellular activity levels and hence the physiological and behavioral events in an oscillatory pattern (Strauss & Dircksen 2010). However, under normal conditions the clock is always exposed to a cyclic environment and the rhythm is driven by external time cues

("*Zeitgeber*", german for time giver). Moreover, reliable environmental cues are required to entrain endogenous rhythms to their 24h period (Pittendrigh C 1981). Because of the constant light/dark period due to the rotation of the earth, light is the most reliable and utilized *Zeitgeber* (Aschoff 1960). In addition to light, temperature, food availability and social cues also act as predominant pacemakers (Aschoff 1960; Roenneberg & Merrow 2005; Gaten et al. 2008; Mauvoisin et al. 2014).

Therefore an adaptation of circadian clocks to the local environment with regard to internal biochemical and physiological processes as well as behavior is possible (Kuhlman et al. 2007). In synchronization with the light-dark cycle, organisms display a significant daily oscillation in metabolic activity such as sleeping, resting or migrating in the water column (Godlewska M. 1996; Roenneberg & Merrow 2005; Gaten et al. 2008; Teschke et al. 2011).

Circadian rhythmicity is also well documented in several crustaceans, e.g. for locomotion, reproduction, sensory organs or the central nervous system such as metabolism and developmental processes (Strauss & Dircksen 2010). The pacemaker of crustacean is, as in many other animals, located in the nervous system (Aréchiga et al. 1993). However, no crustacean single central brain oscillator or master clock could have been identified so far (Strauss & Dircksen 2010). Several neuronal tissues act together in a complex system, which all contain distinct oscillators located in the brain (supraoesophageal ganglion), the retina of the eye, the eyestalks and the caudal photoreceptors (Strauss & Dircksen 2010). Several circadian clock components have been identified. The CLK protein and the PER-like protein was first identified in the prawn *Macrobrachium rosenbergii* and the CRY- like protein in the crayfish *Procambarus clarkii* (Arechiga & Rodriguez-Sosa 1998; Sandeman et al. 1992; Naylor & Emeritus 2010; Aréchiga & Rodríguez-Sosa 2002; Yan et al. 2006).

1.2.3 The circadian clock in *E. superba*

Due to the very advanced research of the circadian system in *Drosophila* and other crustaceans, analogies to the Antarctic krill can be drawn. Mazzotta et al. (2010) identified the cryptochrome (CRY) clock gene (EsCry) in *E. superba* for the first time. It clusters with the insect Cry2 family of *Drosophila* and displayed a 24h oscillation in mRNA expression in the krill head. On the basis of these findings it was the first step toward establishing the presence of an endogenous circadian time-keeping system in krill. In addition, the EsCry2 gene is similar to the gene identified in the monarch butterfly *Danaus plexippus*, whereby one cry gene encodes a fly-like protein with photosensitive properties, while the other encodes a mouse-like protein with potent transcriptional repressive activity (Zhu et al. 2006). On the basis of the findings of Mazzotta et al. (2010),

Teschke et al. (2011) determined transcript levels of cry2 in krill and observed highly rhythmic patterns in gene expression in light-dark 16:8 and constant darkness. In addition, the oxygen consumption oscillates with a period of ~9-12 hours, correlating well with key enzyme activity profiles of citrate CS, trypsin (TRY), aldo-keto reductase (AK) and N-acetylglucosaminidase (NAGase) during light-dark and constant darkness. These results constitute the first report of an endogenous circadian timing system in krill which might be linked to metabolic key processes (Teschke et al. 2011). Recently, Biscontin et al. (2017) suggested that the high level of conservation of the EsCRY1 and EsCRY2 genes and functions indicated that the circadian clock machinery in krill represents an ancestral circadian clock in crustaceans. Furthermore, EsClock, EsCycle, EsPeriod, EsTimeless1 and EsCryptochrome2 could also be identified and showed significantly different, daily rhythmic expression patterns (Biscontin et al. 2008). Laboratory studies of krill indicated that even with the absence of the *Zeitgeber* photoperiod, seasonal changes in metabolic activity (Teschke et al. in preparation) as well as the maturity cycles (Kawaguchi et al. 2007) persist.

Therefore, it might be most likely that biochemical and physiological processes and even behavior of Antarctic krill are controlled by an endogenous circadian timing system. There are already initial indications and findings about these complex mechanisms but in general, the knowledge is still scarce and research is only at the beginning to understand these complex interactions (Mazzotta et al. 2010; Teschke et al. 2011). On the basis of its superordinate role as key species in the food web of the SO it is essential to expand this knowledge for future prediction how Antarctic krill might be affected by the consequences (increasing water temperature, changing sea-ice duration and expand and changing of time for phytoplankton formation) of global warming and whether an adaptation of the endogenous circadian timing system to these changes is possible.

1.3 Aim of the study

The present study aims for a more comprehensive analysis of endogenous circadian regulation in Antarctic krill, especially with regard to possible optimization of the methodological approach to the identification of putative rhythmic gene expression patterns of krill in the laboratory. Previous results often gained a high variance by examining individual biological replicates, as well as a low amplitude of oscillations between the studied time points. In order to optimize these two sources of error, a tissue-specific examination was executed in comparison to previous experiments. The following sub-targets should be investigated within this thesis:

1) detection of putative rhythmic gene expression patterns of clock genes (*clock, cycle, period, timeless, cryptochrome 2, clockwork orange, vrille, E75, doubletime2, shaggy*).

2) tissue-specificity of clock gene expression in different tissues (eyestalks and brain) to identify potential interactions between clock genes and specific tissues.

3) efficiency of different primer sets of *clock* and *timeless* to draw conclusions on the accuracy of clock gene expression quantification in different tissues of krill.

This study provides a basic approach, to understand whether examined genes play a more superordinate role in the eyestalks or brain and if the tissue-specific examination causes more significant patterns of oscillation. The master thesis was investigated within the framework of the Helmholtz Virtual Institute (HVI) Polar Time. In addition to the clock gene expression data generated in this thesis DVM and respirometric data, from another project, were used to describe the relationship between clock gene activities in relation to behavior functions. The krill used for the clock gene expression analysis and the behavior studies are from the same population in the field and reared under same laboratory conditions before they were used for the different experimental approaches. The gene expression patterns examined in this study may provide together with the DVM and respirometric results first insights into the complex interactions between behavior and biochemical processes, regulated a the circadian clock gene machinery, in krill.

2 Material & Methods

2.1 Sampling of *E. superba* in the field and maintenance in the laboratory

E. superba were caught in East Antarctica (66°47'S, 65°08'E) at February 12th, 2013 by a Rectangular Midwater Trawl (RMT 8) in the upper 20-30 metres (m) of the water column during the voyage V3 12/13 with RSV *Aurora Australis* from the Australian Antarctic Division (AAD). On board, krill were maintained in 3 x 200 litres (l), 3 x 100 l and 1 x 50 l tanks. Water was delivered directly to the tanks from the ship's uncontaminated seawater line until the water temperature reached 1°C. The incoming water was then glycol-chilled to 0.5°C until the water flow was stopped completely and the air temperature (0.5°C) kept the water chilled. The krill arrived at the AAD aquarium on February 22th, 2013 and were transferred into 200 l holding tanks. Water temperature (0.5°C) and quality was monitored by a 5000 l seawater recirculation system. A detailed description of the Australian Antarctic Division holding system is described by King et al. (2003). The specimens were fed daily with a mix of live algae (*Geminigera cryophila* (2 x 10^4 cells ml^{-1}), *Phaeodactylum tricornutum* (2.2 x 10^4 cells ml^{-1}), *Pyramimonas gelidicola* (2.4 x 10^4 cells ml^{-1}). A mix of instant algae of 1 x 10^4 cells ml *Thalassiosira weissflogii* (1200TM, CCMP1051/TWsp., Reed Mariculture, USA), 5 x 10^4 cells ml *Isochrysis sp.* (1800TM, Reed Mariculture, USA) and 4.8 x 10^4 cells ml *Pavlova sp.* (1800TM, Reed Mariculture, USA) were added. Krill also received 2 g per tank of nutritional supplements (1 g of Frippak #1 CAR, 1 g of Frippak #2 CAR, INVE, Thailand). After feeding, the water flow was shut off for 2 h to enable the krill to filter-feed on the algal mixture. Using a PC-controlled timer and dimming system (winDIM v4.0e, EEE, Portugal) the light regime in the holding system resembles that of the Southern Ocean. This enables a sinusoidal cycle with monthly variations of the photoperiod and different light intensity during the day by assuming continuous light and a maximum of 100-lux light intensity at the surface of the tank (equal to 1 % light penetration at 30 m depth) during summer midday (December at 66°S). Every month the system was adjusted to simulate the Southern Ocean light conditions.

2.2 Experimental design and sampling

Prior to the experiment (November 29th, 2016, 192 adult krill specimens were transferred from the holding tank into the three experimental tanks (200 l; n=63 in tank A, n=69 in tank B and n=60 in tank C) at 0.5°C. The experiment was started on December 5th, 2016 at 2:00 AM and ended after 80 h on December 8th, 2016 at 10:00 AM (**Fehler! Verweisquelle konnte nicht gefunden werden.** A). Nine krill specimens (three of each tank (A,B,C)) were sampled at 2:00 AM, 6:00 AM, 10:00 AM, 14:00 PM, 18:00 PM and 22:00 PM, respectively (**Fehler! Verweisquelle konnte nicht gefunden werden.** A).

After 24 h under a 12:12 LD photoperiod it was changed to constant darkness (**Fehler! Verweisquelle konnte nicht gefunden werden.** B). During the experiment, feeding was suspended. For the master thesis the samples of the first 28 h were analyzed due to the limited time frame (**Fehler! Verweisquelle konnte nicht gefunden werden.** C).

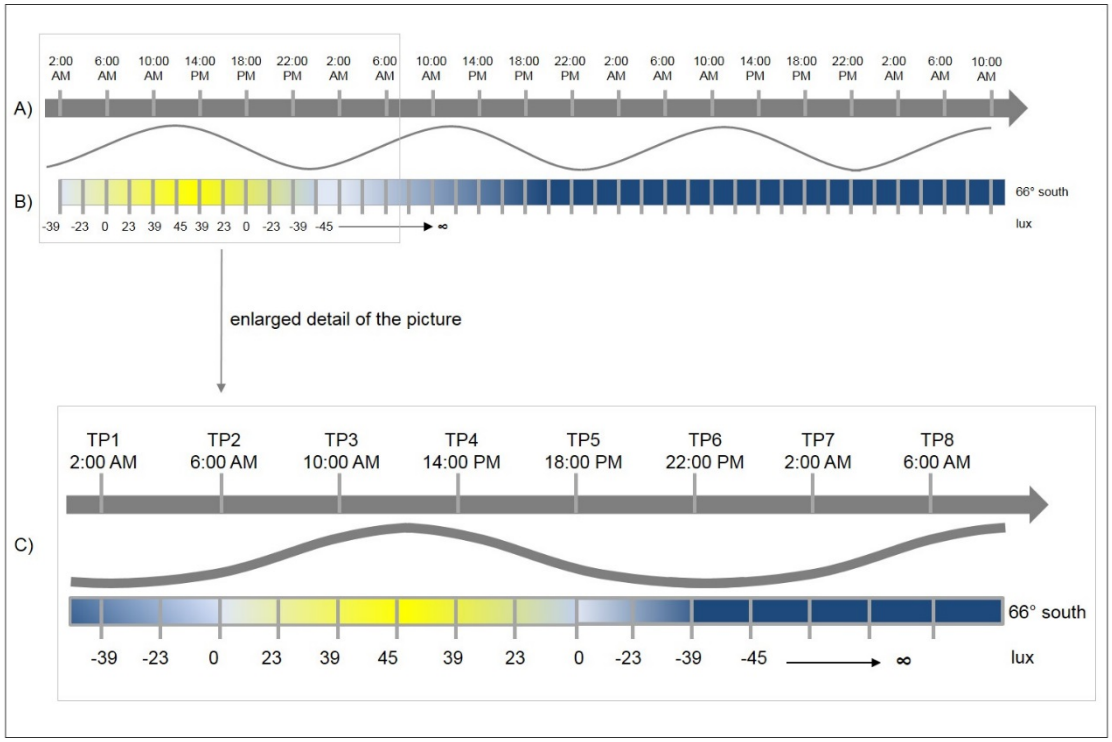

Figure 2 Experimental set up: A) Sampling time points every 4 hours (h) over 80 h. B) Photoperiod in November at 66°south at 30 m depth in lux. The light settings in the aquarium do not go below zero. C) First 28 hours analyzed in the following project.

For the analysis of gene expression in different tissues of the head, a separation of the head from the body was necessary, which was executed with a fine scissors in a skewed angle to cut directly behind the eyes and without the stomach (**Fehler! Verweisquelle konnte nicht gefunden werden.**). In the following, the antennas and the endopods were cut directly behind the eyes. Dissected heads were stored in 1 ml RNAlater™ Stabilization Solution (Thermo Fisher Scientific, USA) in a 2 ml Cryo vial over night at 4°C for fixation. The heads were then cleaned until only eyes, eyestalks and brain were left (**Fehler! Verweisquelle konnte nicht gefunden werden.**A) and then stored at -80°C for later analysis.

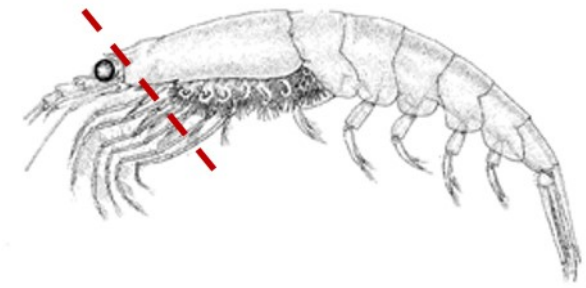

Figure 3 Separation of the head from the body. The head was cut in a skewed angle directly behind the eyes and separated from the rest of the body without the stomach. The red dashed line indicates the section line. [Reference: http://www.fao.org/fishery/species/3393/en]

2.3 Dissection of tissues

Before dissection, the brain, eyestalks and eyes stored at -80°C (see 3.2) were transferred to -20°C to ensure a gentle thawing process. The dissection was performed using a binocular (Leica MZ125) and cooling chambers for Petri dishes. The tissues were dissected into eyes (E), eyestalks (ES) and brain (B), using fine scissors and tweezers. First, the eyes were separated by cutting as close at the transition between eyes and eyestalks as possible (Figure 4B) without contaminating the eyestalks with pigments of the eyes. Leftover pigments on the eyestalks had to be removed thoroughly before RNA extraction to avoid any interference during RNA concentration measurements. The eyestalks were cut as close to the brain as possible (Figure 4**Fehler! Verweisquelle konnte nicht gefunden werden.**C). The brain was cleaned by removing chitin leftovers as well as irrelevant tissues (Figure 4B). The dissected tissues were stored individually in 500 µl RNAlater™ Stabilization Solution at -20°C until RNA extraction.

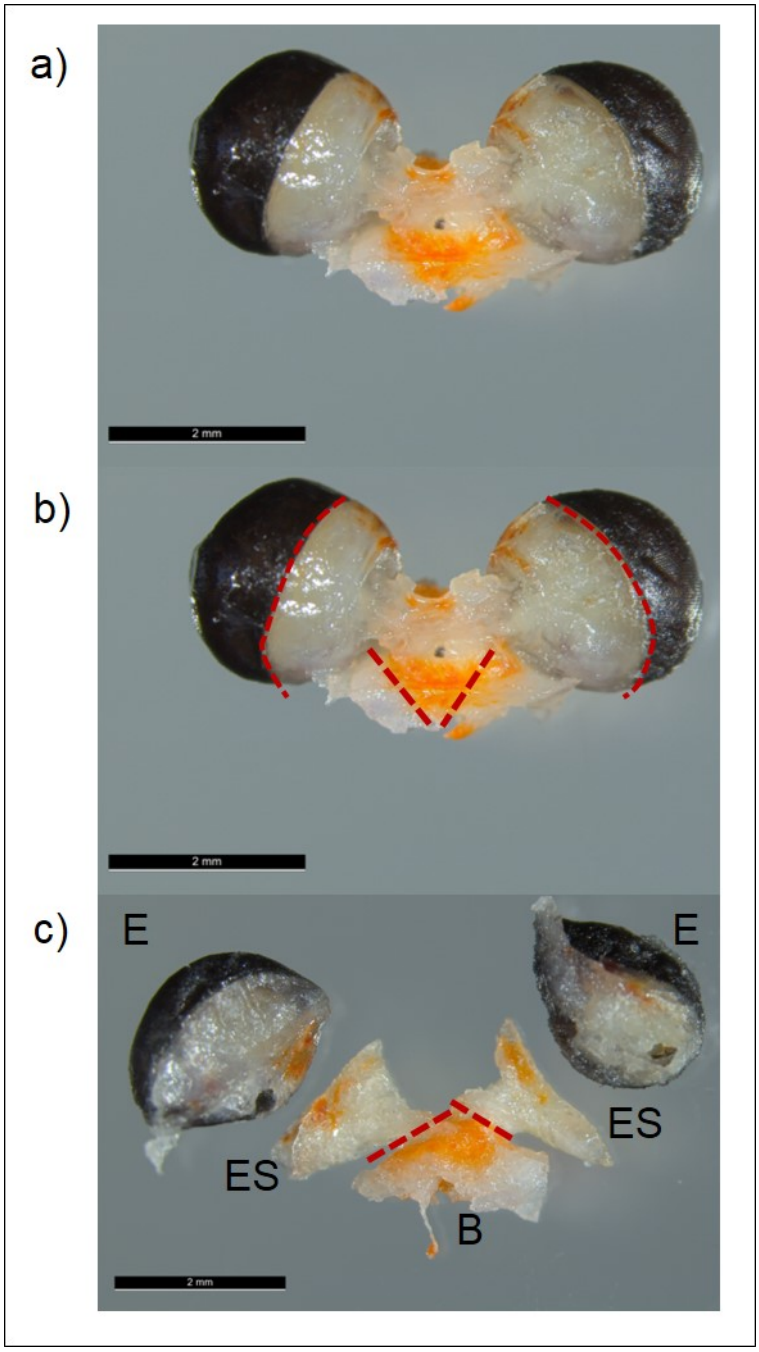

Figure 4 Separation of krill head into specific tissues: a) Exemplary preparation of the connected eyes (E), eyestalks (ES) and brain (B) before separation. b) Separation of eyes without contamination of the eyestalks with pigments of the retina, if possible. Cleaning of brain by removing chitin leftovers as well as irrelevant tissues. c) Separation of eyestalks as close to the brain as possible. Red dashed line indicate the section lines.

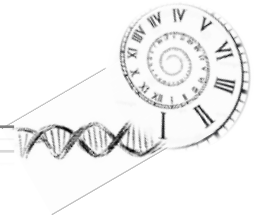

2.4 RNA extraction

To develop and adapt a suitable protocol for RNA extraction of brain and eyestalks tests were necessary. However, for RNA extraction of the eyes, a suitable method could not be established in the brief period of time. The pigments of the retina could not be separated by the extraction columns of the direct-Zol™ RNA Mini Prep Kit (Zymo Research, USA), the NucleoSpin® RNA Kit (Macherey and Nagel), the RNeasy Plus Mini Kit and the RNeasy Lipid Tissue Mini kit (Qiagen). They possibly distort RNA quantification using the Nanodrop 2000 Spectrophotmeter (Thermo Fisher Scientific, USA). Furthermore, purifications using the RNA Clean & Concentrator™-5 (Zymo Research, Irvine, USA) and precipitations with sodium acetate (3M) and lithium chloride (8M) could not provide satisfactory results. RNA of eyestalks and brain were extracted using the direct-Zol™ RNA MircoPrep kit (Zymo Research, USA). For tissue homogenization, 300 µl TRIzol™ Reagent (Thermo Fisher Scientific, USA) was added into 0.5 ml Precellys® tubes containing 1.4 mm ceramic beads. Tissues were dried on KimWipes (Kimberly-Clark Corporation, USA), transferred into the prepared tubes and homogenized immediately by using the Precellys® 24 homogenizer (bertin Technologies, France) for 2x15 seconds (s) at 5000 rpm and 4°C. Homogenates were transferred into 1.5 ml RNase-free Eppendorf® tubes (Eppendorf, Hamburg, Germany) and incubated for 5 minutes (min) at room temperature (RT). 60 µl chloroform (Sigma-Aldrich, USA) was added, the tube securely vortexed and after 3 min incubation at RT centrifuged at 12,000 x g for 15 min at 4°C. The mixture separated into three phases (lower red phenol-chloroform, interphase and a colorless upper aqueous phase containing the RNA). Only the upper colorless aqueous phase was transferred into a new 1.5 ml RNase-free Eppendorf® tube and stored on ice. 50 µl nuclease-free water (Sigma-Aldrich, USA) was added to the remaining mixture, securely vortexed, centrifuged and the resulting upper aqueous phase was removed and again added to the first aqueous phase. An equal volume of 100% molecular biology grade ethanol (AppliChem, Germany) was added and the mixture thoroughly mixed. The mixture was transferred into a Zymo-Spin™ IC column with collection tube and centrifuged at 16,000 x g for 30 s. The column was transferred into a new collection tube and the flow-through discarded. 400 µl RNA Wash Buffer was added to the column, centrifuged and the flow-through was discarded again. For the DNase I treatment in the column a mastermix was prepared (5 µl DNase (6U/µl) and 35 µl DNA digestion buffer) mixed and stored on ice until further use. 40 µl mastermix were added directly to the column and incubated at RT (20-30°C) for 15 min. The column was washed two times by adding 400 µl direct-Zol RNA Prewash Buffer and the flow-through was discarded by pipetting. 700 µl RNA Wash Buffer was added and centrifuged at 16,000 x g for 2 min and the flow-

through discarded again. To ensure the complete removal of RNA Wash Buffer, the column was centrifuged again. To elute the RNA, 15 µl of nuclease-free water were directly added to the column and centrifuged at 16,000 x g for 30 s. The eluate was stored on ice to determine RNA concentration and then stored at -80°C. RNA concentrations and purity were determined by using the Nanodrop 2000 Spectrophotometer. 260/280 ratios of ~2.0 are generally accepted as pure RNA. Furthermore, the 260/230 ratios of pure nucleic acid are often 1.8-2.2 and higher than the 260/280 ratio. For the brain samples the mean 260/280 ratios were 2.04 and 1.88 for the 260/230 ratio. Eyestalk samples had a mean 260/280 ratio of 2.35 and 2.20 for the 260/230 ratio. Integrity of RNA and presence of leftover genomic contamination were tested using the Agilent Bioanalyzer 2100 (Figure 5) and the RNA 6000 Nano Kit (Agilent Technology) according to manufacturer's instructions.

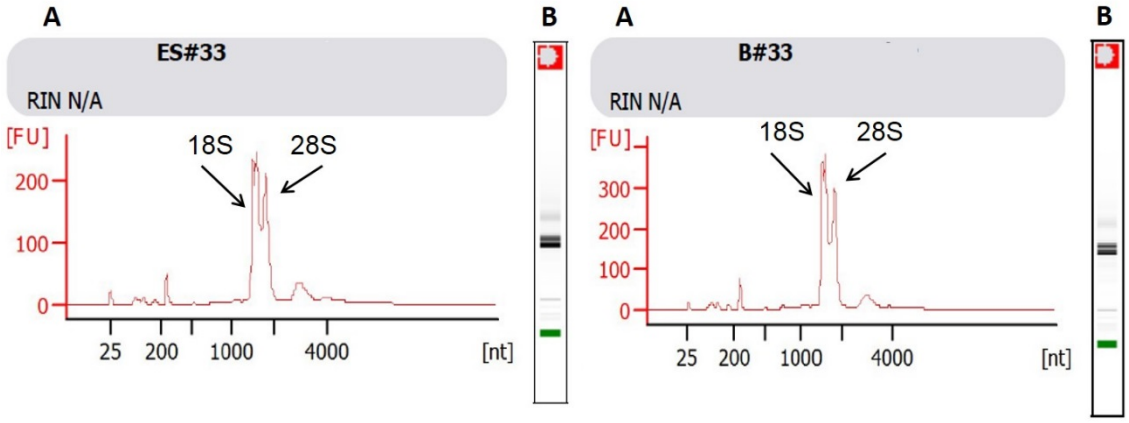

Figure 5 Electropherogram (A) and gel (B) of an exemplary eyestalk (ES) and brain (B) sample of Antarctic krill (*E. superba*): Results of microfluidic electrophoresis in Agilent 2100 Bioanalyzer using the RNA 6000 Nano Kit System. RNA degradation, usually indicated by small smeared peaks within the 200-1000 nt region, and genomic contamination, usually indicated by big bulked peaks within the 2000-4000 nt region, were not present. Time of RNA peak appearance (size related; x-axis) is plotted against the fluorescence (concentration related; y-axis).

2.4.1 Comparison of RNA quantification methods

Due to the potential overestimation of the Nanodrop 2000 Spectrophotometer RNA concentration measurements of the eye samples, the concentrations of the eyestalk and brain samples were additionally measured with the Qubit RNA Broad-Range Assay Kit (Thermo Fisher Scientific, USA). As a result, the accuracy of the Nanodrop 2000 Spectrophotometer should be checked in order to have precise concentration values for the following cDNA synthesis. To determine the absolute difference (%) the

concentration (ng/µl) of the same sample was measured with the Nanodrop 2000 Spectrophotometer (measurements=2) and with the Qubit fluorometer (measurements=3) mean value for each method calculated (Table 1).

Table 1: Comparison of Nandrop 2000 Spectrophotometer and Qubit Fluorometric Quantitation. Calculation of the absolute difference [%] of the mean Nanodrop concentrations (measurements=2) and the mean Qubit concentrations (measurements=3). Samples from the eyestalk (ES) and brain (B) were used.

Sample #	mean [Nanodrop [ng/µl]]	mean [Qubit [ng/µl]]	absolute difference [%]
ES#2900	249.85	255.00	2.02%
ES#2908	445.55	439.00	1.49%
ES#2907	417.55	408.00	2.34%
ES#2910	427.20	446.00	4.22%
ES#1856	636.50	671.00	5.14%
ES#2904	494.05	532.00	7.13%
ES#1850	261.30	289.33	9.69%
ES#1852	265.45	280.00	5.20%
ES#1848	273.85	283.00	3.23%
ES#1847	240.10	268.33	10.52%
B#2902	72.75	72.33	0.58%
B#1841	112.60	129.67	13.16%
B#1845	81.25	73.83	10.05%
B#2910	137.65	139.33	1.21%
B#1856	92.95	96.60	3.78%
B#1846	108.05	105.43	2.48%
B#1842	109.30	105.33	3.77%
B#1847	143.95	149.33	3.60%
B#1850	129.00	120.33	7.20%
B#2909	184.25	185.67	0.76%

Due to the low mean in the absolute difference (4.88 %) and the large number of RNA extraction in this study, concentrations were measured with the Nanodrop 2000 Spectrophotometer.

2.5 Validation of spike controls

Besides using an internal control or housekeeping gene which itself may show fluctuations in expression levels, an exogenous target sequence control was spiked into the sample RNA during cDNA synthesis for an accurate normalization of gene expression. The exogenous target sequence controls (spikes) were selected from a human transcript plasmid library and generated by cooperation partners at the Department of Biology of the University of Padova (Padova, Italy). Spikes were added to each sample at a constant concentration.

2.5.1 Spike transcription, purification and quality control

3 µg dry pellet of linearized plasmids of six different spikes (Spike 5, Spike 6, Spike 15, Spike 18, Spike 20, Spike 25) were re-suspended in 20 µl nuclease-free water by gentle vortexing. The suspensions were stored over night at 4°C. 1.5 µg of DNA were transcribed into RNA using the MAXIscript™ T3 Transcription Kit (Thermo Fisher Scientific, USA). 20 µl of total volume for one reaction included 10 µl of re-suspended spike and 10 µl of the mastermix for one reaction (2 µl 10 x transcription buffer, 1 µl 10 mM ATP, 1 µl 10 mM CTP, 1 µl 10 mM GTP, 1 µl 10 mM UTP, 2 µl T3 enzyme mix and 2 µl nuclease-free-water). The mixture was gently pipetted up and down, briefly microfuged and incubated for 1 h at 37°C. 1 µl TURBO DNase™ was added, mixed well and incubated for 15 min at 37°C. 30 µl nuclease-free water was added to a final volume of 50 µl. The transcripts were purified using the RNA Clean & Concentrator™-5 (Zymo Research, Irvine, USA). 100 µl RNA Binding Buffer was added, mixed and 150 µl 100% molecular biology grade ethanol was added. After mixing, the sample was transferred to the Zymo-Spin™ IC column and centrifuged for 30 s at 12,000 x g. 400 µl RNA Prep Buffer was added and the flow-through discarded by pipetting. The same procedure was repeated using 700 µl RNA Wash Buffer. 400 µl RNA Wash Buffer was added and centrifuged for 2 min. The flow-through was discarded and the column centrifuged again for 30 s to ensure the removal of the RNA Wash Buffer.10 µl nucelase-free water was added directly to the column and centrifuged for 30 s. The concentration and purity of the eluted RNA was immediately measured using the Nanodrop 2000 Spectrophotometer and then stored at -80°C. Additionally, the integrity of the RNA and the presence of contamination was checked with the Agilent Bioanalyzer 2100 (Figure 6).

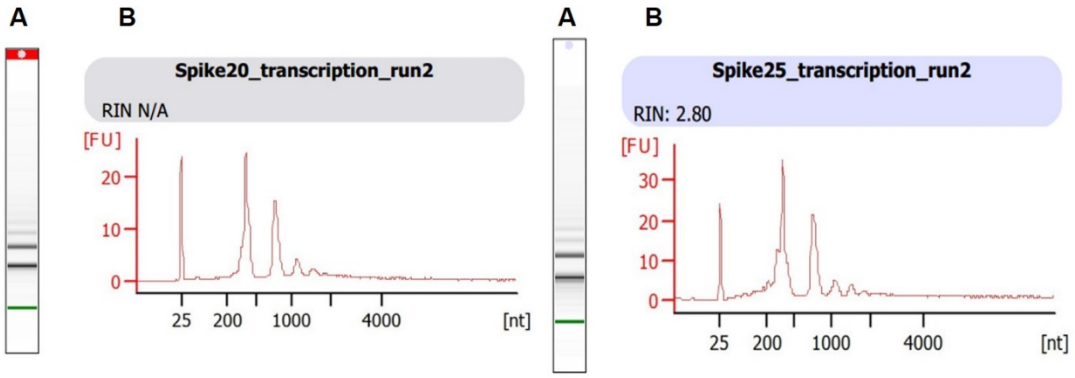

Figure 6 Gel (A) and electropherogram (B) of the spikes 20 and 25 for *E. superba*: Results of microfluidic electrophoresis in Agilent 2100 Bioanalyzer using a RNA 6000 Nano Kit System. Time of RNA peak appearance (size related; x-axis) is plotted against fluorescence of the peak (concentration related; y-axis). The peak at 25 nt is the lower marker of the RNA 6000 Nano Kit System and the peak around 220 [nt] is the spike. All electropherograms showed the same peak pattern (750 nt, 1000 nt and 1800 nt) which might be a result of non-completed digestion. These peaks do not affect the analysis. For a more precise evidence, sequencing is necessary.

2.5.2 Real-time PCR (qPCR) titration curves of spike controls and cDNA amplification without spike control

In order to establish the optimal spike control as well as spike concentration for the final analyses, real-time quantitative PCR (qPCR) titration curves were implemented. A dilution series of each spike transcript was prepared (10 ng, 1 ng, 100 pg, 10 pg, 1 pg) and cDNA synthesis was performed adding 1 µl of the different spike dilutions (for cDNA synthesis protocol see 2.6 cDNA synthesis). For each qPCR reaction, 5µl of 1:5 diluted cDNA (4 ng/µl) were added to 4 µl nuclease-free water, 1 µl primer mix (forward and reverse (360 µl, 20x mix) of the spike control or clock-gene) and 10 µl 2x TagMan® Gene Expression Master Mix for a final reaction volume of 20 µl. For each cDNA sample, three technical replicates were added on a 96-well reaction plate and relative abundance of target RNAs was measured using the ViiA™ 7 Real-Time PCR System (Thermo Fisher Scientific). The PCR 96-well reaction plate was sealed, briefly vortexed and centrifuged. Reaction conditions were as follows: 1 cycle of stage 1 with 50°C for 2 min and 95°C for 10 min, 40 cycles of stage 2 with 95°C for 15 s and 60°C for 1 min. In addition to the samples, no template controls (NTC) and no reverse transcription controls (-RT) were added to each plate. In the NTCs, nuclease-free water instead of RNA template was used during cDNA synthesis to identify putative contaminations of the RT-qPCR Master Mix. Reliable results of the NTCs should only display background noise or have high Ct (cycle threshold) values as a result of primer-dimer formation. In the -RT controls, the

enzyme reverse transcriptase is omitted during cDNA synthesis, thus preventing the synthesis of cDNA in the sample. The –RT control allows the identification of genomic DNA contamination. In case of contamination, genomic DNA gets amplified during qPCR and Ct values similar to that of samples may be obtained. For the analysis of the samples and to compare between data obtained from different genes and qPCR runs, the baseline threshold for all qPCR runs were set to 0.1. For each spike, the logarithmic mean Ct value of each concentration step was plotted and the slope used for the calculation of primer efficiency. Due to the results of the RT-qPCR and considering the efficiencies, 10 pg of spike 20 (efficiency: 87.5%) and spike 25 (efficiency: 89.8%) were used for further analysis. Furthermore, this concentration exhibited similar Ct values compared to test runs with known clock-genes (**Fehler! Verweisquelle konnte nicht gefunden werden.**B) and therefore, seemed appropriate. To exclude unspecific binding of the spike primer sequences to the cDNA templates, qPCR was performed without the addition of spike primers (**Fehler! Verweisquelle konnte nicht gefunden werden.**C).

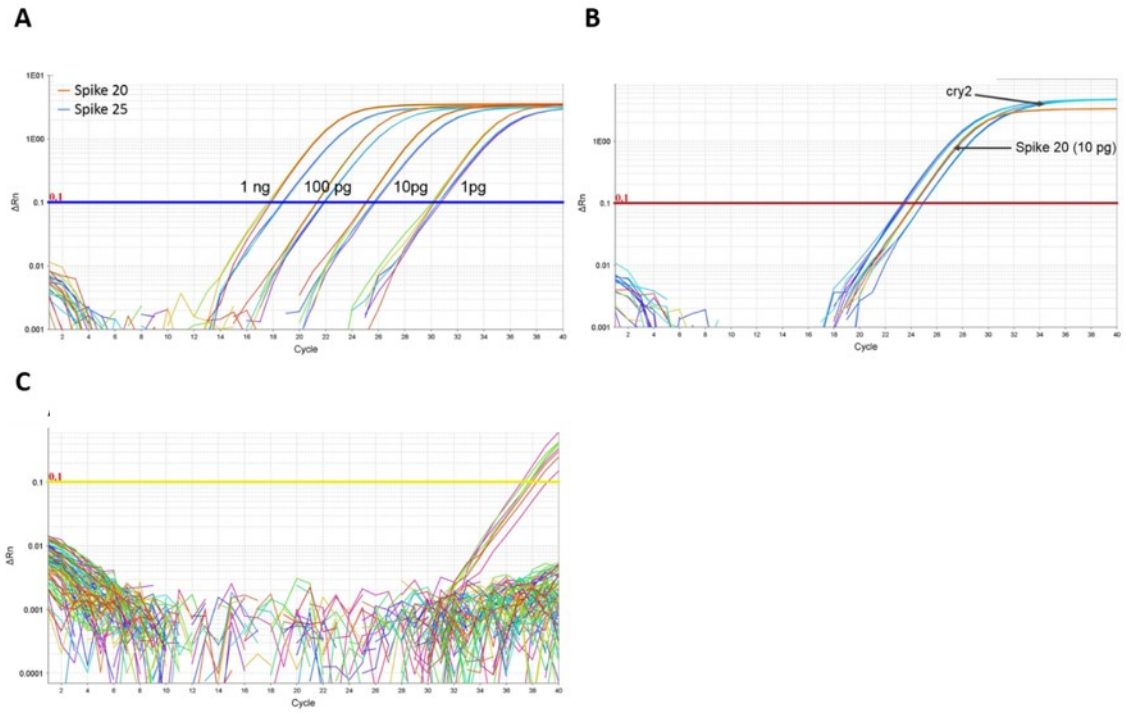

Figure 7 Amplification plots of the TaqMan® Real-Time PCR-Assays. (A) Amplification plot of the spike controls 20 and 25 with different concentrations (1 ng,100 pg, 10 pg, 1 pg). (B) Amplification plot of spike control 20 (10 pg) and the chryptochrome 2 gene (cry2). (C) Specification of spikes: qPCR was performed without the addition of spike primers

2.6 cDNA synthesis

The extracted RNA has to be reverse transcribed into cDNA. For cDNA synthesis 5 µl of the spike 20 and spike 25 mastermix (2 pg/µl) and 23.25 µl of RNA (1 µg RNA was diluted with RNase-free water) and 21.75 µl of mastermix (10 µl 5 x buffer, 1 µl dNTPs (10 mM), 0.5 µl RNase I (40 U/µl), 5 µl RNase-free water, 5 µl pentadecamere (500 µM) and 0.25 µl reverse transcriptase; Thermo Fisher Scientific Molecular Biology) were mixed (total volume: 50 µl). After mixing and centrifuging, the RNA was reversely transcribed to cDNA with the T100™ Thermal Cycler (Biorad). NTCs were included on each cDNA synthesis plate. As the total amount of RNA was too small to allow for –RT controls, they were conducted using test RNA from similar krill samples to exclude DNA contamination. The cDNA synthesis was performed at 25°C for 10 min, 37°C for 50 min, 70°C for 15 min and cDNA was stored at -20°C for further analysis. Due to low RNA concentration for a couple of samples not all 9 biological replicates for each time point (TP) could analyzed. Consequently, for the ES samples (TP1 n=8; TP2 n=7; TP3 n=8; TP4 n=8; TP5 n=8; TP6 n=9; TP7 n=9; TP8 n=9) and for the B samples (TP1 n=8; TP2 n=8; TP3 n=8; TP4 n=9; TP5 n=8; TP6 n=9; TP7 n=9; TP8 n=9) were reverse transcribed into cDNA.

2.7 Preparation of the Custom TaqMan® Array Card and TaqMan® Gene Expression Assays

2.7.1 Gene selection for TaqMan® Gene Expression Assay

Based on already published data (Teschke et al. 2011; Mazzotta et al. 2010; Tomioka & Matsumoto 2015; De Pittà et al. 2013; Hardin 2005; Hunt et al. 2017) the regulatory genes *clock (clk)*, *cycle (cyc)*, *period (per)*, *timeless (tim)*, *cryptochrome 2 (cry2)*, *clockwork orange (cwo)*, *vrille (vri)*, *E75*, *doubletime 2 (dbt2)* and s*haggy (sgg),* all involved in the first major regulatory loop of the insect circadian clockwork (**Fehler! Verweisquelle konnte nicht gefunden werden.**) were selected. *Ubiquitin specific peptidase 46 (USP46)* was selected as endogenous control (housekeeper). The sequences of the genes were obtained from the Krill database (http://krilldb.bio.unipd.it/) (Sales et al. 2017). Besides using an endogenous control (

Table 2) the exogenous target sequence controls (spike20; XM_017004857.1 and spike 25; XM_011537537.1) were chosen.

2.7.2 Sequence verification

The selected target gene sequences for the Custom TagMan® Array Card were checked using the Basic Local Alignment Search Tool (BLAST) of the National Center for Biotechnology Information (NCBI; https://www.ncbi.nlm.nih.gov). BLASTN and BLASTX search were used to verify the selected sequences. Additionally, they were verified against the krill-specific sequence database (http://krilldb.bio.unipd.it; Sales et al. 2017). Besides this, the reading frame of each target sequence was examined and was converted if necessary using the web-based tool *Reverse complement* (https://www.bioinformatics.org/sms/rev_comp.html). Furthermore, low-complexity regions and repeats were masked using the web-based tool *RepeatMasker* (http://www.repeatmasker.org). A 150 nucleotide part close to the 3' end of each target sequence without low-complexity regions and repeats was then selected and cut using *EMBOSS seqret* (http://www.ebi.ac.uk/Tools/sfc/emboss_seqret). Afterwards, processed target sequences were loaded into the Custom TaqMan Assay Design Tool from Thermo Fisher Scientific (https://www.thermofisher.com/order/custom-genomic-products/tools/gene-expression/) for automatic primer design. After primer design, assay IDs were created and inserted into the format of the Custom TaqMan® Array Card (

Figure 8). For primer sequences of target genes, housekeeping genes and spike controls used for RT-qPCR, see

Table 2.

Format 16 (Cat. No. 4346798)
15 unique assays + 1 mandatory control
8 unique samples

Replicates	1	2	3	4	5	6	7	8	9	10	11	12	13	14	15	16	17	18	19	20	21	22	23	24	Port
1	1	1	1	2	2	2	3	3	3	CTL	CTL	CTL	4	4	4	5	5	5	6	6	6	7	7	7	A
	8	8	8	9	9	9	10	10	10	11	11	11	12	12	12	13	13	13	14	14	14	15	15	15	B
2	1	1	1	2	2	2	3	3	3	CTL	CTL	CTL	4	4	4	5	5	5	6	6	6	7	7	7	C
	8	8	8	9	9	9	10	10	10	11	11	11	12	12	12	13	13	13	14	14	14	15	15	15	D
3	1	1	1	2	2	2	3	3	3	CTL	CTL	CTL	4	4	4	5	5	5	6	6	6	7	7	7	E
	8	8	8	9	9	9	10	10	10	11	11	11	12	12	12	13	13	13	14	14	14	15	15	15	F
4	1	1	1	2	2	2	3	3	3	CTL	CTL	CTL	4	4	4	5	5	5	6	6	6	7	7	7	G
	8	8	8	9	9	9	10	10	10	11	11	11	12	12	12	13	13	13	14	14	14	15	15	15	H
5	1	1	1	2	2	2	3	3	3	CTL	CTL	CTL	4	4	4	5	5	5	6	6	6	7	7	7	I
	8	8	8	9	9	9	10	10	10	11	11	11	12	12	12	13	13	13	14	14	14	15	15	15	J
6	1	1	1	2	2	2	3	3	3	CTL	CTL	CTL	4	4	4	5	5	5	6	6	6	7	7	7	K
	8	8	8	9	9	9	10	10	10	11	11	11	12	12	12	13	13	13	14	14	14	15	15	15	L
7	1	1	1	2	2	2	3	3	3	CTL	CTL	CTL	4	4	4	5	5	5	6	6	6	7	7	7	M
	8	8	8	9	9	9	10	10	10	11	11	11	12	12	12	13	13	13	14	14	14	15	15	15	N
8	1	1	1	2	2	2	3	3	3	CTL	CTL	CTL	4	4	4	5	5	5	6	6	6	7	7	7	O
	8	8	8	9	9	9	10	10	10	11	11	11	12	12	12	13	13	13	14	14	14	15	15	15	P

Figure 8 Custom TaqMan ® Array Card format used in this study. Instead of the slot of the mandatory control (CTL) another gene was loaded. [Reference: http://www3.appliedbiosystems.com/cms/groups/mcb_marketing/documents/generaldocuments/cms_040127.pdf].

Table 2: Primer sequences of target genes, housekeeping genes and spike controls used for RT-qPCR. The sequences of the genes were taken from the Krill database (http://krilldb.bio.unipd.it/) (Sales et al. 2017).

Target gene		**Primer sequence (‘5-‘3)**	**Accession number**
clock_F	fwd	GGCCTCAGTTGGTACGAGAAATG	ESS034514
	rev	AATTTCCATTCTATACTGTGCCTTGATGT	
clock_A	fwd	GCAGCGTCAGCTTCAAGAG	ESS034514
	rev	GCTGTTGTCGCATTATCATTTGCT	
cycle	fwd	GCAGGATCAGATTGTGCGTCAA	ESS133965
	rev	TGCTATCTACACAGGAAGCTCTTCT	
period	fwd	TGAGGGTAAATTCAACAATAAATGGAATACATCT	ESS133963
	rev	GAGTAACATCAACATTTTCCAACCAACT	
timeless_F	fwd	CAAGACAAAGCGAGATGGCATTT	ESS040526
	rev	AGGGTTGGAAGAAGGTTTTGTGAAA	
timeless_A	fwd	CAGCTTGTGCTCCATGGAAAAC	ESS040526
	rev	CTTAGGCAGTTGATGTAAGATCATGTCT	
cryptochrome 2	fwd	CAGTGCTCAAGAACTTCCCAACTAA	FM200054, Mazzotta et al 2010
	rev	GTCCTATGACACATTTAGACTGT	
clockwork orange	fwd	AAAACTTTGATAAACAAAACCTCTTTCATC	ESS049812
	rev	GAGGGAGCTCATGACATGTGT	
vrille	fwd	GAAGTAGCTACACTTAAATACCTGTTGGT	ESS123359
	rev	CAAAACTATTCTAACGAGATCCATCGGA	
E75	fwd	CAGTCTGCTTCTGCTTCAACCT	ESS094384
	rev	GCCTTCTGACGGTGCTCTAC	
doubletime 2	fwd	AAAGAATAGAGCTTCAATATGTATATATTTAAAACAAAGT	ESS096455
	rev	TGAAAACAAGAAAAATTATAGAATCTTCTATCCTAGATAAGG	
shaggy	fwd	GGTGGGTTGCGGAACATTG	ESS074789
	rev	TGGTCCACCACTGCCA	
adenosine triphosphate-γ	fwd	GTCAAGAACATCCAGAAGATCACTCA	ESS108986
	rev	GCTTCAACTCCCTTTCAGCTCTT	
Housekeeping gene		**Primer sequence (‘5-‘3)**	
ubiquitin specific peptidase 46	fwd	TGGAACTGGTATTAACAGAGGACACT	ESS079224
	rev	CTGCATCGTCATCAAAGAGCA	
Spike control		**Primer sequence (‘5-‘3)**	
Spike 20	fwd	TGCAATGATGATAACCGTTCCCTTTAA	XM_017004857.1
	rev	CCAGATATGCTTGAATTGGATCACCT	
Spike 25	fwd	GCTGGGACCTAGTGTCAAGTAC	XM_011537537.1
	rev	TGGAGTAACCATGCTAGATTAAAGAAATACAATT	

2.7.3 TaqMan® Gene Expression Assays

For TaqMan® Gene Expression Assay, 100 µl of total volume per reaction (20 µl of the cDNA (20 ng/µl) and 30 µl of RNase-free water and 50 µl of the TaqMan® mastermix) was prepared in a 1.5 ml Eppendorf tube. The tubes were shortly centrifuged. For each reaction, 98 µl were slowly added into the well of the corresponding sample-loading port. The TaqMan® card was centrifuged two times at 1,200 rpm for 1 minute. The card was inserted into the sealer and each well was closed. Loading-ports were removed using a scissor and the card loaded into the Vii-A7 Real-Time PCR System (Thermo Fisher). For analysis and to maintain comparability between data obtained from different genes and runs, the machine-aided relative threshold for all qPCR runs was set. Due to technical problems (power failure) one TaqMan® card, loaded with cDNA samples from the brain, was excluded from the analysis. Consequently, for the analysis of the gene expression the following biological replicates of the brain (TP1 n=7; TP2 n=7; TP3 n=6; TP4 n=8; TP5 n=7; TP6 n=7; TP7 n=7; TP8 n=7) and of the eyestalks (TP1 n=8; TP2 n=7; TP3 n=6; TP4 n=8; TP5 n=8; TP6 n=9; TP7 n=9; TP8 n=9) were analyzed.

2.8 Data analysis

2.8.1 Data quality control

To assess the expression stability of the housekeepers, mean raw Ct-values were plotted over time (see Figure 9a). Overall, the level of the raw Ct-values were higher in the eyestalks compared to the brain. Except for ZT4, housekeeper mRNA expression was stable over time and showed very little variation within both tissues (Figure 9a). At ZT4, expression peaked and showed very high standard errors in both tissues in Spike 20, Spike 25 and *Usp46*. In order to obtain stable housekeepers for expression normalization, biological replicates were compared among each other at ZT4 (Figure 9b). At ZT4 3 samples with extraordinarily high values could be identified as outliers according to Nalimov ((Lozán & Kausch 1998); brain: TP3_B#32;eyestalks:TP3_ES#32 and TP3_ES#41) and removed from the data set. After removal, housekeeper expression was stable the in both tissues (Figure 10). Technical errors as well as biological variations between krill individuals could have accounted for the difference in expression in these three samples.

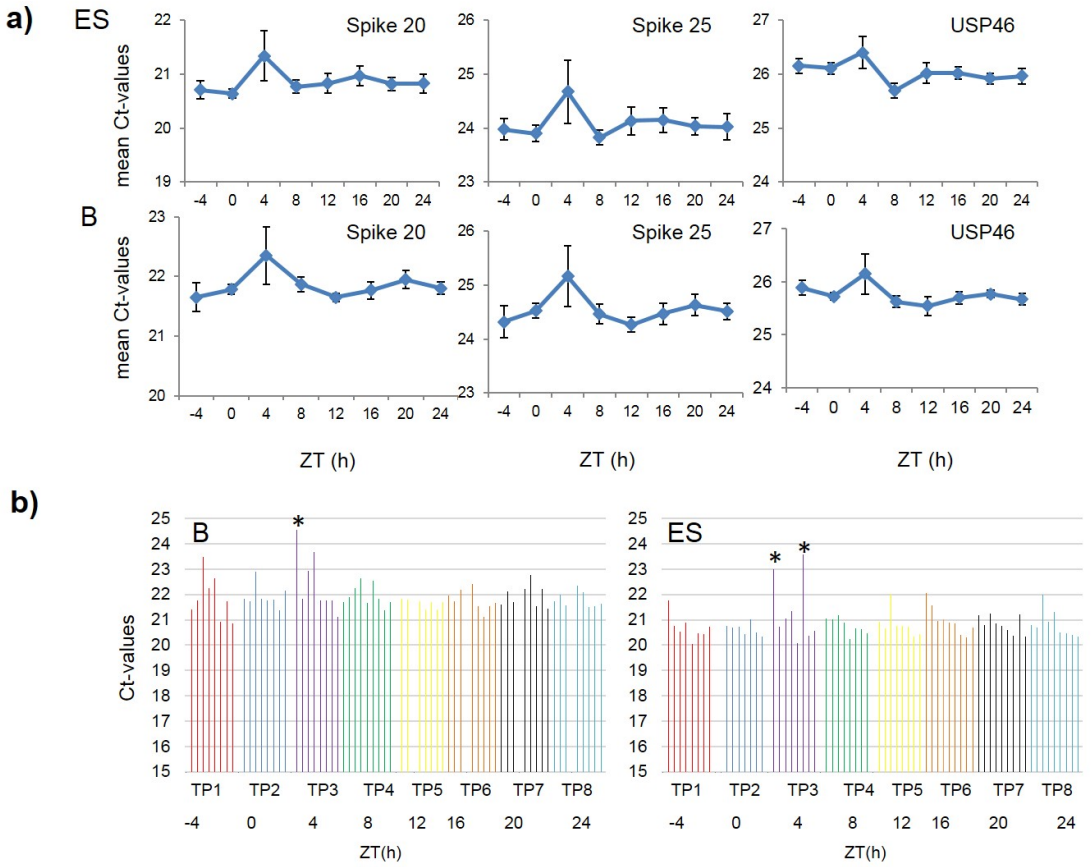

Figure 9: Raw Ct-values of endogenous and exogenous housekeepers. ZT = *Zeitgeber* Time, indicating the time intervals from the beginning of the light phase (x-axis) plotted against raw Ct-values of (y-axis). a) Raw mean Ct-values of the endogenous (*Usp46*) and exogenous housekeepers (Spike 20 and Spike 25) in eyestalks (ES) and brain (B). Data are expressed as mean ± SEM (n=6-9). b) Raw Ct-values for each biological replicate at different time points (TP), exemplary for Spike 20, in eyestalks (ES) and brain (B). Stars indicate outliers.

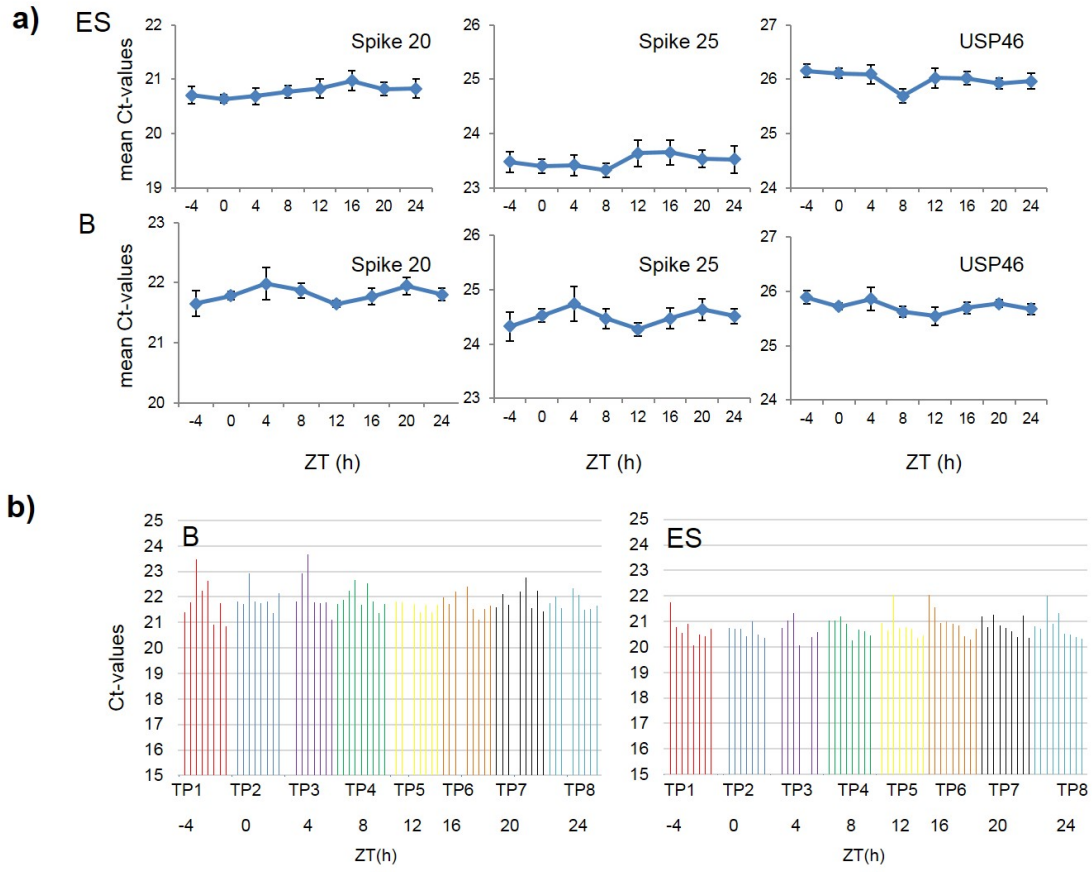

Figure 10: Raw Ct-values of endogenous and exogenous housekeepers after outlier removal. ZT = *Zeitgeber* Time, indicating the time intervals from the beginning of the light phase (x-axis) plotted against raw Ct-values (y-axis). a) Raw mean Ct-values of the endogenous (*Usp46*) and exogenous housekeepers (Spike 20 and Spike 25) in eyestalks (ES) and brain (B). Shown is the mean ± SEM (n=6-9). b) Raw Ct-values for each biological replicate at different time points (TP), exemplary for Spike 20, in eyestalks (ES) and brain (B).

2.8.2 Selection of housekeepers/reference genes

For normalization, a combination of *Usp46* and one of the exogenous target sequence genes was used. To assess the most stable combination of exogenous controls (Spike 20, spike 25) and *Usp46*, the geometric mean of the combinations (*Usp46* + Spike 20; *Usp46* + Spike 25) was calculated and plotted over time (Figure 11). The combination of *Usp46* and Spike 20 expression was more consistent over time in both tissues compared to Spike 25. Furthermore, the NormFinder software in R identified the combination of Spike 20 and *Usp46* as most stable (Andersen et al. 2004). Therefore, the combination of *Usp46* and Spike 20 was used as reference.

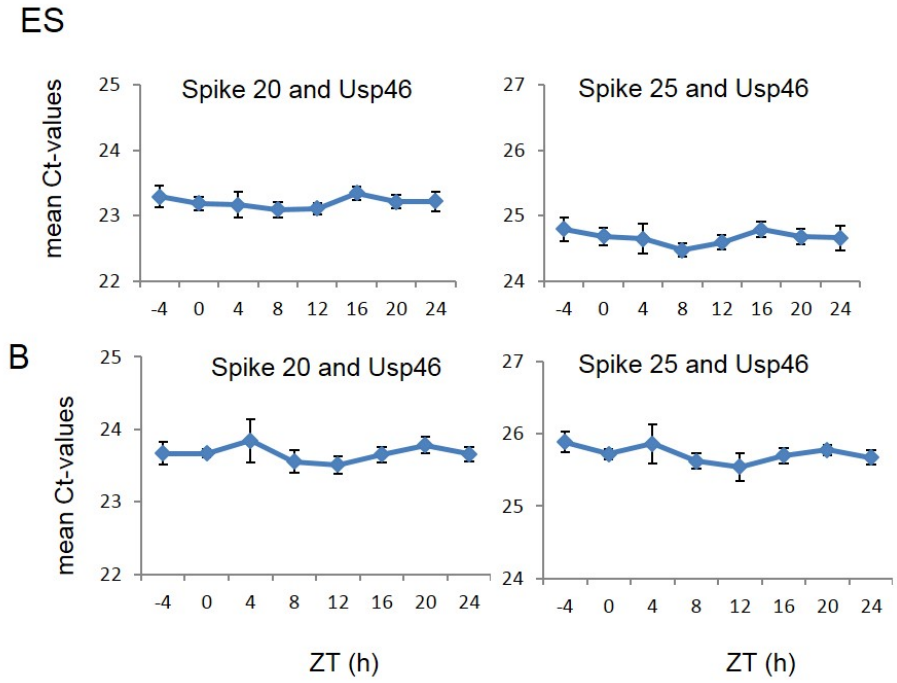

Figure 11: Geometric mean of raw Ct-values of endogenous and exogenous control. ZT = Zeitgeber Time, indicating the time intervals from the beginning of the light phase (x-axis) plotted against the geometric mean of raw Ct-values (y-axis). Upper panel: Combination of Spike 20/ Spike 25 + Usp46, respectively in eyestalks (ES). Lower panel: Combination of Spike 20/ Spike 25 + Usp46, respectively in brain (B). Data are expressed as geometric mean ± SEM (n=6-9).

2.9. Normalization and relative quantification

A combination of *Usp46* and Spike20 were used as reference for normalization of gene expression. Normalized relative quantities (NRQs) were calculated according to Hellemans et al. (2007). Scaling of raw Ct-values (calculation of relative quantities; RQs) was performed for each tissue separately as well as across both tissues to maintain tissue-specific expression levels.

2.10 Statistics

For statistical analysis the RStudio (R Core Team (2017). R: A language and environment for statistical computing. R Foundation for Statistical Computing, Vienna, Austria) package RAIN (Thaben & Westermark 2014) was used to identify putative 24 h rhythmicity in daily patterns of gene expression. For each tissue, data were adjusted in a 24h period to a sinusoidal curve by expressing the probability of consistency by p-values and the phases of the sinusoidal curve (amplitude of the oscillation is maximal). The p-values were then corrected for multiple comparison using the *false discovery method (fdr)* of Benjamini, Hochberg, and Yekutieli (Benjamini & Hochberg 1995;

Benjamini & Yekutieli 2001) implemented within the package. For each tissue, Kruskal–Wallis non-parametric ANOVAs followed by multiple t-tests corrected for multiple comparisons (Bonferroni method) were applied to test for differences between time points within a gene.To compare gene expression levels between eyestalk and brain tissues for each time point (TP), non-parametric Mann-Whitney-Wilcoxon tests were used. Significant differences between tissues at the respective TP are indicated by hash keys.

3 Results

3.1 Primer efficiency of *timeless* and *clock*

By comparing the two primer pairs for *Clk* in brain, it became visible that the relative NRQ levels for *Clk_F* displayed higher expressed compared to *Clk_A* (Figure 13) although, expression patterns were not-significant and similar for both primer pairs. In the eyestalks, the patterns of *Clk_F* and *Clk_A* showed a trend to even greater consistency over time (Figure 13). The comparison of *Tim*_F and *Tim_A* primers in the brain revealed similar expression patterns for both primer pairs, despite higher mRNA levels for *Tim_F* (Figure 13). In the eyestalks, the pattern displayed less consistency for *Tim* primer pairs and also higher NRQ levels in *Tim_A*.

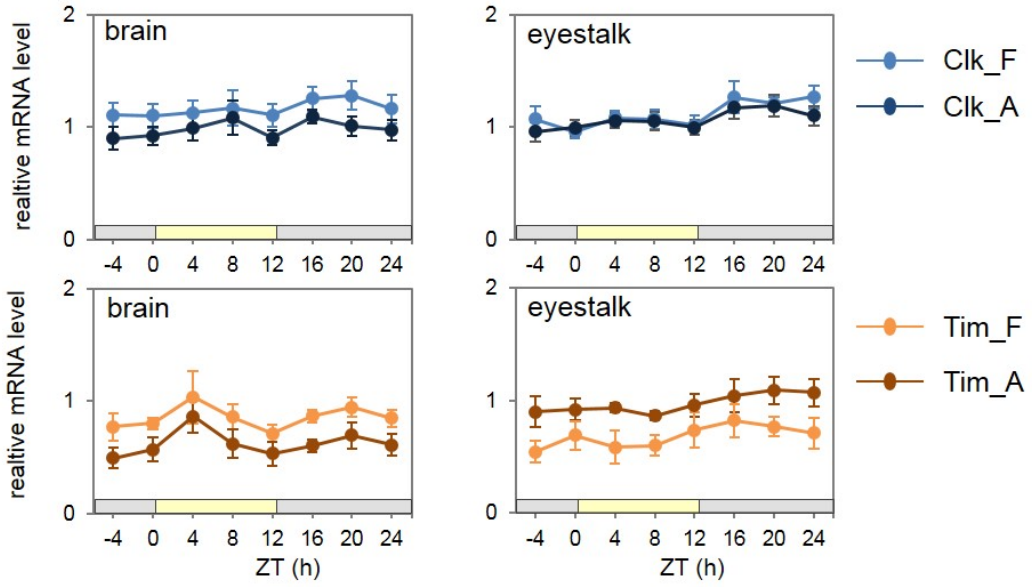

Figure 12: Relative mRNA levels using different primer sets of *clock* and *timeless*. Relative mRNA level plotted against *Zeitgeber*-Time (ZT), indicating the sampling intervals from the beginning of the light phase in brain and eyestalk, respectively. Data are expressed as mean ± SEM (n=6-9). Grey (= dark phase) and yellow (= light phase) bars beneath the graph indicate the respective photoperiod. From ZT24, experimental light conditions remained at constant darkness.

To compare efficiencies of the two different primer sets for *timeless* and *clock*, Ct-values were plotted against the logarithm of the dilution series/logarithm of CDNA concentrations (100 ng, 200 ng, 400 ng, 800 ng) (see Figure 13). Values for the correlation coefficient (R^2) were close to 1 (0.9785 to 0.9996) (see Figure 13).

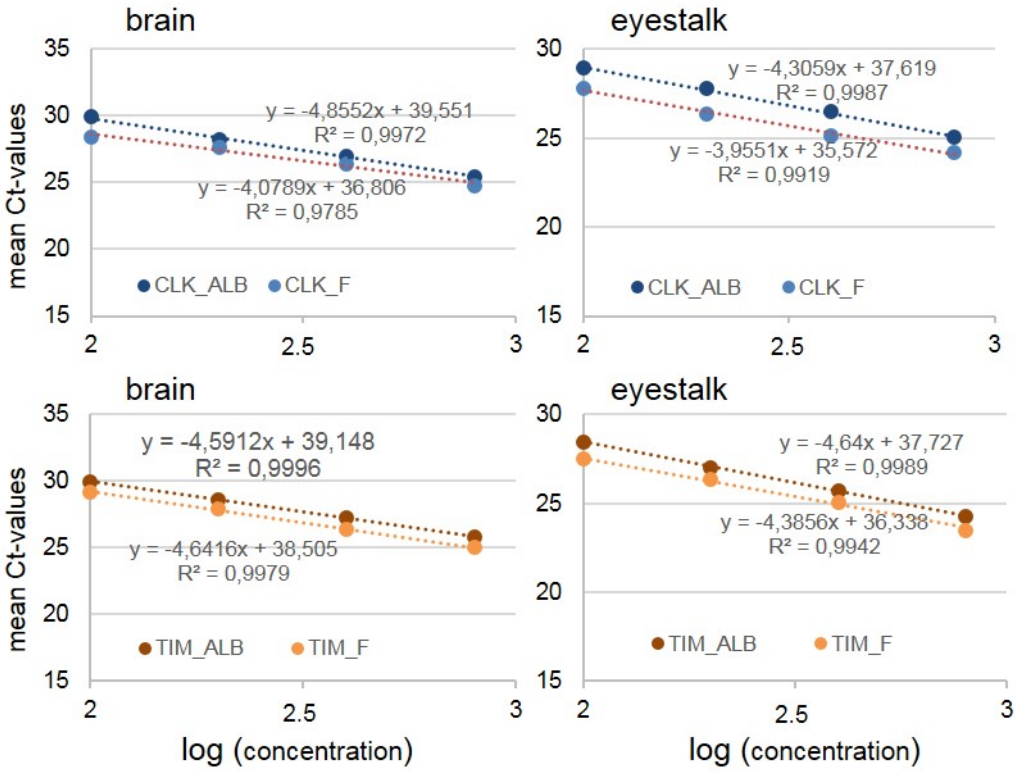

Figure 13 Primer efficiency using different primer sets. Ct-values of different primer sets of *Clk* and *Tim* were plotted against the logarithm of cDNA concentration used in the dilution series (100 ng, 200ng, 400ng and 800ng) in brain and eyestalks, respectively.

Efficiencies were calculated for each primer pair using the formula
$E = (10^{(-1/slope)} - 1) \times 100$. Good primer pairs should have an efficiency between 90% and 110%, hence calculated efficiencies (Table 3) are below the acceptable range. By comparing the different efficiencies, *Clk_F* and *Tim_F* primers indicated significantly higher efficiencies in both tissues compared to *Clk_A* and *Tim_A*.

Table 3: Primer efficiencies: Efficiencies for each primer pair in eyestalks (ES) and brain (B), respectively. Efficiency (E) was calculated according to (www.thermofisher.com/primerefficiency) using the formula E = (10^(-1/slope) -1) x 100.

	primer	efficiency (%)
brain	*Tim_A*	82.56
	Tim_F	82.11
	Clk_A	80.34
	Clk_F	87.93
eyestalk	*Tim_A*	82.13
	Tim_F	84.53
	Clk_A	85.35
	Clk_F	89.50

Based on the higher primer efficiency of the *Clk_F* and *Tim_F* primer pairs in brain and eyestalks (Table 3) and considering the similarity of mRNA expression patterns between the different primer pairs/sets for *Clk* and *Tim* (Figure 12), only *Clk_F* and *Tim_F* primer pairs were used for further analyses.

3.2 Regulatory network of clock gene expression patterns

Correlation of clock gene expression was visualized using hierarchical clustering in both, brain and eyestalks. In brain, daily mRNA expression patterns of *Per*, *Clk*, *Cyc* and *Vri* as well as *Sgg*, *Cwo* and *E75* and finally, *Cry2*, *Tim* and *Dbt* were correlated (Figure 14**Fehler! Verweisquelle konnte nicht gefunden werden.**a). Besides the similarity of gene expression the heat map visualized for *Vri* highest expression levels at TP1, for *Tim* highest expression at TP3 and for *Per*, *Cyc*, *Sgg*, *Cwo*, *E75* and *Cry2* highest expression at TP6 and for *Clk* and *Dbt* highest values at TP7.

In eyestalks (Figure 14**Fehler! Verweisquelle konnte nicht gefunden werden.**b) clock genes clustered in a different way compared to brain. *Cyc*, *Vri*, *Tim*, *Per* and *Clk* gene expression patterns were correlated. *Sgg*, *E75* and *Dbt* as well as *Cry2* and *Cwo* daily expression patterns showed high similarities. Besides the similarity of gene expression the heat map visualized highest values at TP6, TP7 and TP8 during darkness. *Sgg* showed also highest expression values in the first dark phase at TP2.

By comparing the gene expression patterns of both tissues, in the eyestalks the heatmap visualized that the genes more correlated with each other. Moreover, in eyestalks gene expression pattern showed higher levels during dark phase (TP6-TP8) compared to brain.

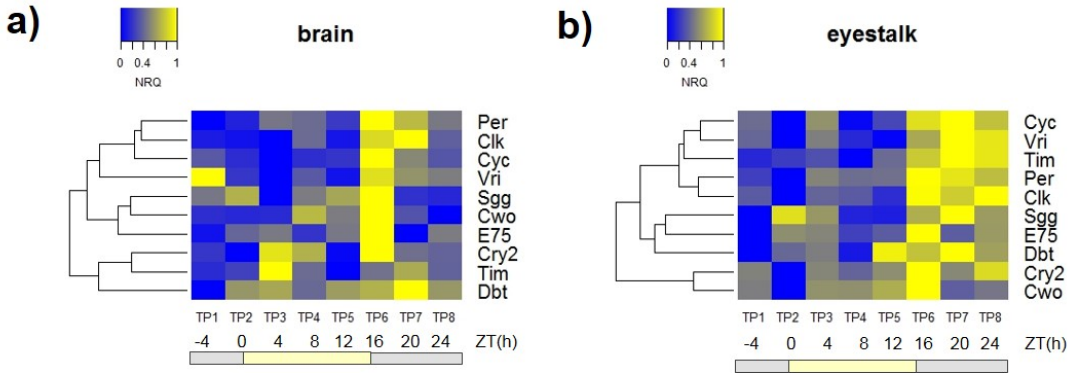

Figure 14 Heat maps of daily clock gene expression patterns in brain and eyestalks. a) Clock gene expression (Clk, Cyc, Dbt, Per, Tim, Sgg, Cry2, Cwo, E75 and Vri) over time (28h) in brain. b) Clock gene expression (Clk, Cyc, Dbt, Per, Tim, Sgg, Cry2, Cwo, E75 and Vri) over time (28h) in eyestalks (for more details on clock gene regulatory network see Figure 1). Genes clustered together based on the similarity of daily gene expression patterns.

3.3 Daily profiles of clock gene expression in brain and eyestalks

3.3.1 Within tissues

A similar pattern could be observed for *Clk* in brain (range from 1.10 to 1.17) and eyestalk (range from 0.96 to 1.08) (Figure 15a). The increase during dark phase (ZT12-24) is more remarkable in eyestalks (increase of 0.25) compared to brain (increase of 0.18). For *Cry2,* two maxima could be identified over time, reaching the first peak at ZT4 and the second peak at ZT16 in both tissues (Figure 15b). Again, relative mRNA levels in eyestalks showed a more distinct increase during dark phase. In the eyestalks, relative mRNA levels of *Cwo* increased from ZT4 to ZT16 (increase of 0.18) followed by an abrupt decrease (Figure 15c) whereas in brain two maxima could be identified at ZT8 and ZT16, respectively. As can be seen in Figure 15d, relative mRNA levels of *Cyc* remained constant from ZT-4 to ZT12 in brain (range from 0.90 to 1.08) and peaked at ZT16 (4h after nightfall). In contrast, two maxima could be determined at ZT4 and, at ZT16 (dark phase) with much higher levels, in the eyestalks. Furthermore, daily oscillations of *Cyc* showed a significant period of 24h in both tissues (p=0.029). The daily expression pattern of *Dbt* showed two maxima for both, brain and eyestalk (Figure 15e). At ZT0/ZT4, when lights were switched on as well as at ZT12, when lights were switched off, higher mRNA levels could be detected. Only within the eyestalks, Kruskal–Wallis non-parametric ANOVAs followed by multiple t-tests corrected for multiple comparisons (Bonferroni

method) indicated significant differences TP1-TP7 (p=0.042) (Table 6). A similar pattern could also be identified for *E75* in both tissues (Figure 15f). Relative mRNA levels increased from ZT0 to ZT4 and increased again at ZT16 until lights were switched off. For *Per*, an almost identical expression pattern over time was measured in both tissues (Figure 15g). mRNA levels increase from ZT0 to ZT4 (brain: increase of 0.14; eyestalk: increase of 0.22) after the light was switched on, decreased in the following and increased again to a second peak with highest levels at ZT16 (brain: 1.29; eyestalk: 1.28). Only within the eyestalks, Kruskal–Wallis non-parametric ANOVAs followed by multiple t-tests corrected for multiple comparisons (Bonferroni method) indicated significant differences TP2-TP6 (p=0.0083) and TP2-TP7 (p= 0.042) (Table 6). *Sgg* showed two peaks, one smaller at ZT0 (brain:0.89; eyestalk:1.07) when the light was switched on, in both tissues (Figure 15h). However, in eyestalks the increase started from ZT16, increasing slowly up to ZT20 and then slowly decreased whereas in the brain, mRNA expression abruptly decreased at ZT16. Relative mRNA expression pattern of *Tim* were different between eyestalks and brain (Figure 15i). In brain, levels increased until peaking at ZT4 (1.03), followed by a decrease up to ZT12 (0.71) and another slight increase up to ZT20 (0.95). Compared to brain, mRNA levels in the eyestalks did not display the first peak and a constant increase starting at ZT8 during constant darkness could be determined. In brain, daily patterns of *Vri* displayed highest expression levels during night (ZT-4 (0.75) and ZT12 (0.70)) (Figure 15j). In eyestalks, *Vri* peaked at ZT4. Afterwards, levels decreased and again, increased at ZT12 with a peak at ZT20 (0.91). Furthermore, for *Vri* expressed in brain and eyestalk, a significant daily pattern (p= 0.029) with a 24h period could be observed. Only within the eyestalks, Kruskal–Wallis non-parametric ANOVAs followed by multiple t-tests corrected for multiple comparisons (Bonferroni method) indicated significant differences TP7-TP2 (p=0.024 and TP7-TP5 (p= 0.019) (Table 6).

3.3.2 Between tissues

For each gene analyzed, relative mRNA levels for each time point (TP) were compared among each other in eyestalk and brain tissue (see Figure 15). In general, relative mRNA levels *in Clk, Cry2, Cwo, E75, Per, Tim* and *Vri* were expressed in the same way in both tissues. For *Cyc* and *Sgg* only separate TP indicated significant variations between both tissues (Figure 15d,h). Even measured mRNA levels in *Cyc* evinced significantly higher values in brain at ZT0 (p-value: 0.02622), ZT8 (p-value: 0.01476) and ZT14 (p-value: 0.01111). In comparison, relative mRNA levels in *Sgg* indicated significantly higher values at ZT20 (p-values: 0.01111) and ZT24 (p-values: 0.002468) in the eyestalks. In Figure 15e, it can be seen that over the entire time series, with the exception of ZT12,

significantly higher mRNA levels in the brain could be measured for *Dbt* (p-values of 0.001243 (ZT-4), 0.01107 (ZT0), 0.002165 (ZT4), 0.001088 (ZT8), 0.007898 (ZT16), 0.01111 (ZT20) and 0.0274 (ZT24)).

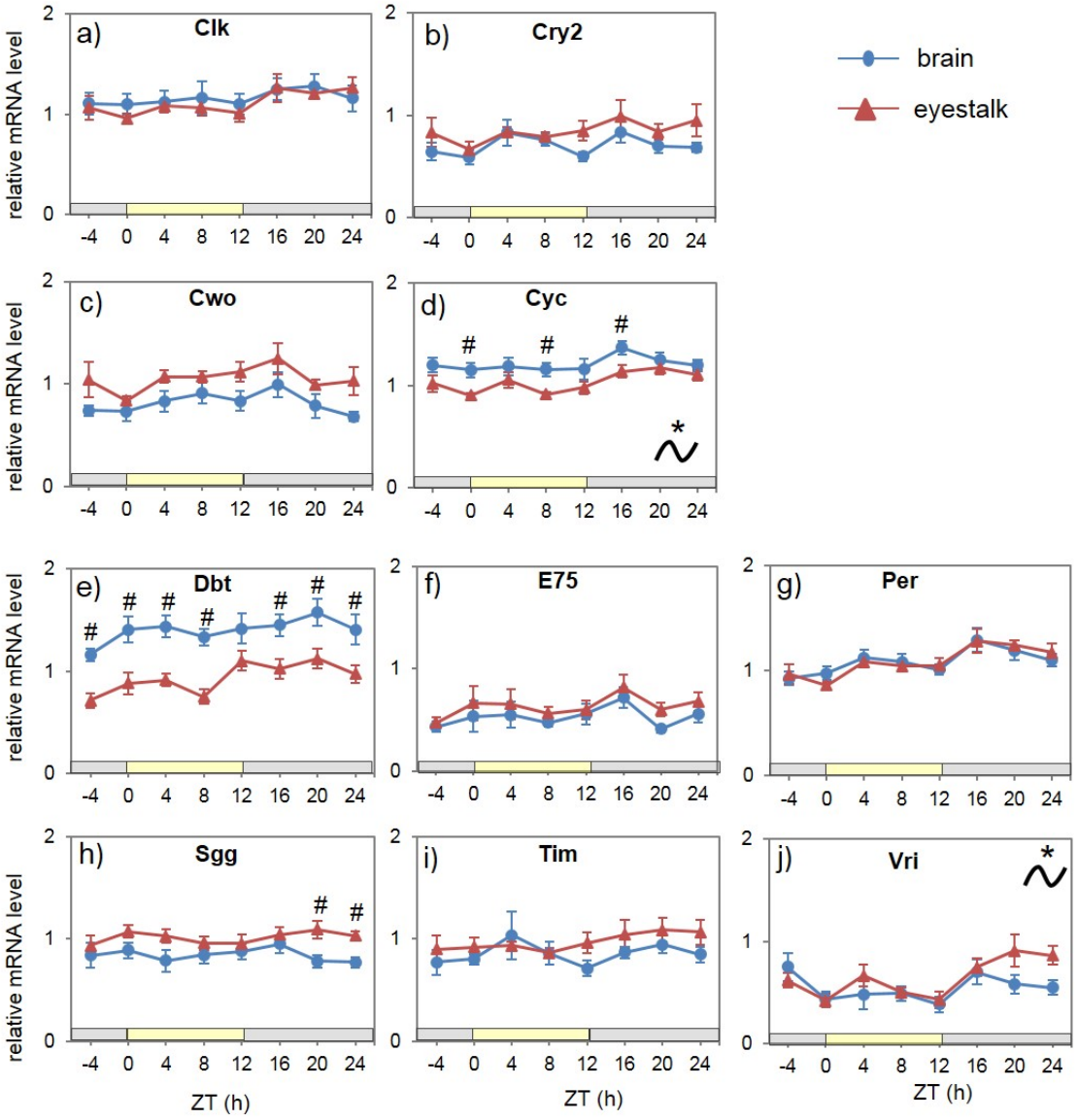

Figure 15: Clock gene expression patterns in brain and eyestalks. Ten clock genes (*Clk, Cry2, Cwo, Cyc, Dbt, E75, Per, Sgg, Tim* and *Vri*) were analyzed over 28h. Relative mRNA level (NRQ) are plotted against ZT = *Zeitgeber* Time, indicating the time intervals from the beginning of the light phase. Data are expressed as mean ± SEM (n=6-9). Grey (dark) and yellow (light) bars beneath the graph indicate the respective photoperiod. Black asterisks and schematic sinus curve indicate significant daily oscillation with a period of 24h in eyestalks and brain determined by RAIN analysis (for p-values see appendix). Hash keys indicate significant differences between both tissues tested for

each ZT (Whitney-Wilcoxon test). From ZT24 onwards, experimental light conditions remained in constant darkness.

3.4 Potential co-regulation of clock genes within and between brain and eyestalks

Schematic representation of the relative mRNA level maxima in brain and eyestalks. Within the brain, *Cyc* and *Clk* showed highest relative mRNA levels around ZT16. Similar expression pattern could also be shown for *E75, Per* and *Cry2*, with maxima around ZT4 and ZT16. The maxima of the relative mRNA levels of *Cwo* (maxima: ZT8; ZT16)*, Dbt* (maxima: ZT4; ZT20*), Sgg* (maxima: ZT0; ZT16) and *Tim* (maxima ZT4; ZT20), were shifted by a 4 hours period before or after ZT4 and ZT16. As the only exception, *Vri* were shifted by 8 hours period, with reference to ZT4 and ZT16, with maxima around ZT-4 and ZT16. Within the eyestalks, *Cyc* and *Per* showed highest relative mRNA levels around ZT4 and ZT16. *Dbt* (maxima: ZT4; ZT20)*, Sgg* (maxima: ZT0; ZT20*), Tim* (maximum: ZT20) and *Vri* (maxima ZT4; ZT20), were shifted by a 4 hours period before or after ZT4 and ZT16. A shift of up to 8 hours, with reference to ZT4 and ZT16, have been showed *Clk* (maximum: ZT17), *Cry2* (maxima: ZT-4; ZT16), *Cwo* (maxima: ZT-4; ZT16) and *E75* (maxima: ZT3; ZT20). Comparing maxima of relative mRNA levels between tissues, similar patterns could be determined for *Clk, Dbt, E75* and *Per* in brain and eyestalks. In contrast, *Sgg* has been showed a shift in maxima of 4 hours between the tissues. For *Cry2, Cwo* and *Vri*, maxima of relative mRNA levels were shifted by 8 to 12 hours between brain and eyestalks. For *Tim*, the eyestalks indicated a less pronounced pattern, therefore the maximum in the brain at ZT4 is no longer present. *Cyc*, behaved the other way round, with double peak at ZT4 and ZT16 in the eyestalks, though the first peak is no longer present in the brain. RAIN analysis (tested periods: 4, 8, 12, 24), only indicated significant 24 hours periods for *Cyc* and *Vri* in brain and eyestalks (Figure 15d,j). However, detection limits of RAIN should not be excluded, as the regular shift of 4 hours between genes is no particular case.

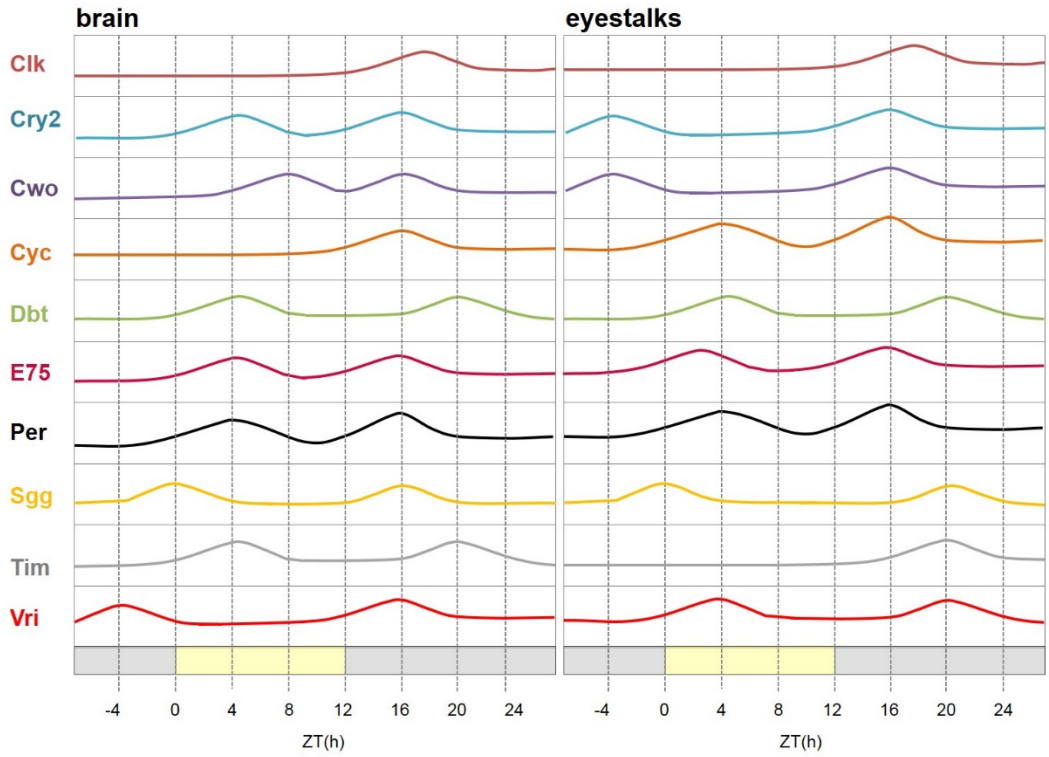

Figure 16: Schematic representation of clock gene expression over time. Relative mRNA expression levels of *Clk, Cry2, Cwo, Cyc, Dbt, E75, Per, Sgg, Tim* and *Vri* in brain and eyestalks were analyzed over 28h and plotted against ZT = *Zeitgeber* Time. Peaks only show when the genes have reached their highest relative mRNA levels. Values on y-axis can not be equated with relative mRNA levels. Grey (dark) and yellow (light) bars beneath indicate the respective photoperiod.

4 Discussion

Recent studies provided information's on the existence of an endogenous timing system in krill that governs metabolic and physiological output rhythms (Mazzotta et al. 2010; Teschke et al. 2011; De Pittà et al. 2013; Biscontin et al. 2017). The present study aimed to identify potential circadian clock gene (*clock, cycle, period, timeless, cryptochrome 2, clockwork orange, vrille, E75, doubletime, shaggy*) expression patterns as well as methodological optimization to reduce gene expression variability and enhance the detection of potential oscillation patterns in Antarctic krill (*E. superba*).

4.1 Regulatory network of clock genes in *E. superba*

The present *Drosophila* circadian clock model consists of three major regulatory loops. One of the core oscillatory loops is based on the interaction of the products of *Clk* and *Cyc* genes. By forming a heterodimer they activate the transcription of *Per* and *Tim* during late day to early night (Tomioka & Matsumoto 2015). Thus, *Per* and *Tim* mRNA levels increase almost in synchrony at late day to early night (Tomioka & Matsumoto 2015). A similar expression pattern could also be identified in the monarch butterfly (Zhu et al. 2008). An upregulation of *Per* at the beginning of the night could be shown in the head of the pea aphid *Acyrthosiphon pisum,* held under the same photoperiod (Cortés et al. 2010). By the same course of *Per* relative mRNA levels in both tissues, it can be concluded that expression seemed to play the same role in both tissues, in *E.superba* (Figure 15g). In brain of *E. superba*, synchronized expression of *Per* and *Tim* could not be detected in brain (Figure 14a). In addition, only *Per* showed an trend of increased relative mRNA levels during night, compared to the entire course of the day (Figure 14a, Figure 15g). In contrast in the eyestalks, the correlation of *Per* and *Tim* is more pronounced (Figure 14b). Besides clustering of *Per* and *Tim*, only *Per* indicated a significant increase ($p= 0.0083$; 0.0289, see Table 6) of mRNA levels during night (TP6 and TP7) compared to early day (TP2) (Figure 14b, Figure 15g). In the eyestalks of the norway lobster (*Nephrops norvegicus)* held under same light conditions, mRNA expression of *Tim* and *Per* increased during day with maximum levels at the end of the day (Sbragaglia et al. 2015). However, in *E. superba* eyestalks, synchronized gene expression patterns of *Tim* and *Per* seemed to be more pronounced, moreover *Per* indicated higher gene expression during night, which shows agreement with literature in *Drosophila* and *A. pisum* (Tomioka & Matsumoto 2015; Cortés et al. 2010).

PER and TIM proteins did not accumulate to peak levels until late evening (Hardin 2005). This delay is elicited due to phosphorylation dependent destabilization of *Per* by *Dbt,* followed by stabilization of phosphorylated *Per* by *Tim* binding (Price et al. 1998).

In krill brain and eyestalks, *Dbt* indicated two maxima, starting during the night with highest values 4 hours after the light is on, and a second maximum starting at the end of the day with highest values during the night. Only in the eyestalks, significantly differences (p=0.042, see Table 6) between 2AM (TP1) and 2AM (TP7) could be determined. Comparing *Dbt* and *Per* within both tissues, it can be shown that both maxima of *Dbt* coursed always 4 hours after the maxima of *Per.* It is very vague to correlate the measured relative mRNA levels between *Dbt* and *Per*, in order to make a statement whether mRNA levels of *Dbt* may have resulted lower expression of *Per* and how the 4 hour shift between *Dbt* and Per might be related to *Dbt* as suppressor.

Rhythmic oscillations in mRNA expression of *Cyc* were already shown in the honey bee as well as in aphids, where *Cyc* mRNA levels increased at the beginning of the dark phase (Rubin et al. 2006; Cortés et al. 2010). A significant rhythmic 24 hour-oscillation of *Cyc* mRNA expression could also be identified in krill brain and eyestalks (Figure 15d). A trend of increasing relative mRNA levels could also be determined at the beginning of the dark phase, more pronounced in eyestalks. However, this trend is not supported by statistics analysis, as no significant difference between the times points could be determined in either tissue.

In the butterfly head, relative mRNA levels of *Cry2* slightly increased during the day with highest levels at the end of the light phase (Zhu et al. 2008). Previous studies on Antarctic krill heads by Teschke et al. (2011) already showed highly rhythmic mRNA expression patterns of *Cry2* under a 16:8 light:dark (LD) regime with an upregulation starting in the morning until the midday. As can be seen in Figure 14a,b, in brain and eyestalks, *Cry2* indicated a trend of higher relative mRNA levels during darkness, more pronounced in the eyestalks. However, no significant differences could be identified between the time points for either tissue, so that our results do not show oscillatory rhythms and agreement with results from Teschke et al. (2011). Moreover, it had to be considered that a direct comparison between the data of Teschke et al. (2011) and our data is not possible because the animals were kept under a different light regime. Due to involvement of *Cry2* in the first major loop, synchronized expression patterns with *Per* and *Tim* could be revealed in the monarch butterfly (Zhu et al. 2006). In krill brain, *Cry2* and *Tim* mRNA expression patterns were correlated (Figure 14a), indicating for *Cry2* highest relative mRNA levels at ZT4/ZT8 and ZT16, and for *Tim* highest levels at ZT4 and ZT20. Relative mRNA levels in krill eyestalks indicated a similar pattern for *Tim* and *Per,* however no direct correlation with *Cry2* (Figure 14b). In summary, it can be said that only in eyestalks there are similarities between *Cry2* and *Tim*. Nevertheless, *Cry2* indicated no clear oscillatory pattern therefore a comparison with *Tim* and *Per* is not possible.

A distinct feedback loop in *Drosophila* controls the rhythmic mRNA expression of *Clk*, activated by *PDP1e* (Tomioka & Matsumoto 2015). *Clk* transcription levels oscillated in an antiphase to *Per* and *Tim*, with peaking transcription levels in the early day (Tomioka & Matsumoto 2015; Amrein & Bray 2003). In the honey bee (*Apis mellifera*) brain, *Clk* relative mRNA levels increased at nightfall (Rubin et al. 2006). However, it is also known that the temporal pattern of gene expression in the honey bee brain is strikingly distinct from the patterns observed in Drosophila. Previous studies of brain and eyestalks in crustaceans indicated that *Clk* mRNA is not expressed in a circadian rhythm (Strauss & Dircksen 2010). Comparing krill's relative mRNA levels of *Clk* in brain and eyestalks, levels coursed relatively constant over time and show no significant differences between the time points. Within both tissues, *Clk* indicated no antiphase to *Per* and *Tim*, due to similar patterns (Figure 14a,b), as described in Drosophila (Tomioka & Matsumoto 2015; Amrein & Bray 2003). Consequently, our results show agreement with data from Crustaceans (Strauss & Dircksen 2010), which leads us to the conclusion that *Clk* probably show no endogenous oscillatory rhythms in krill.

Besides the genes composing the main feedback loop in *Drosophila,* several other genes (*Vri, Cwo, Sgg* and Dbt) are known to be necessary for the rhythmic expression of *Clk* or the modification of the oscillatory loop.

Cortés et al. (2010) showed an increase of *Vri* relative mRNA levels in the head of the pea aphid (*A. pisum)* at nightfall. A significant rhythmic 24 hour-oscillation of *Vri* mRNA expression could also be identified in krill brain and eyestalks. However, only *Vri* in eyestalks indicated a significant increase ($p = 0.024$; 0.019, see Table 6) of mRNA levels during night 2AM (TP7) compared to 6AM (TP2) and 6PM (TP5) (Figure 14b, Figure 15j). *Vri* is expressed in *Drosophila* circadian pacemaker cells in the head and oscillates in the same pattern like *Per* and *Tim*, regulated by the transcription factors CLK and CYC (Blau & Young 1999; Glossop et al. 2003). In krill brain, results of the heat map indicated no agreement between *Vri, Tim* and *Per.* Within the eyestalks, high agreement between *Vri, Tim* and *Per* could be shown with highest relative mRNA levels after the light was switched off, as described in existing literature of *Drosophila* and *A. pisum* in the head (Blau & Young 1999; Glossop et al. 2003; Cortés et al. 2010).

Cwo transcription is directly induced by CLK-CYC, and repressed by PER-TIM in *Drosophila. Cwo* mRNA expression is ryhtmically expressed in the fly head peaking very closely with *Per* and *Tim* (Matsumoto et al. 2007). In krill, the course of *Cwo* relative mRNA levels showed no significant pattern, only a trend of increase during the day with peaking 4 hours after the light is off, followed by decrease during night (Figure 15c). Within brain and eyestalks in krill, *Cwo, Per* and *Tim* indicated no correlation (Figure

14a). Considering the results of krill, no clear oscillatory pattern as well as correlation to *Per* and *Tim* could be detected.

In summary, correlations between relative mRNA levels of the clock genes analyzed in krill, indicated less pronounced or different patterns compared to *Drosophila* and other model organisms. Within the eyestalks of krill, correlations between clock genes are more pronounced and indicate more agreement with literature. Clear 24h oscillatory patterns could be only identified in *Cyc* and *Vri* in brain and eyestalks. Significant differences between time points within a gene, we only determined in eyestalks for *Per*, *Dbt* and *Vri.* This results and the more pronounced correlations within the eyestalks, visualized in the heat maps, leads us to the conclusion that clearer results of potential oscillatory rhythms can be identified in krill's eyestalks. Nevertheless, as the knowledge about clock genes in crustacean is still at the very beginning, compared to the fruit fly and monarch butterfly, yet it is not clear whether the regulation in krill might be work in a different way.

4.1.2 Comparison of relative *mRNA levels* in brain and eyestalks

In crustaceans, the brain (supraoesophageal ganglion), the retina of the eye, the eyestalk and the caudal photoreceptor are already identified as an important part of circadian regulation (Strauss & Dircksen 2010). The brain photoreceptors could be identified to be necessary for light entrainment but the endogenous rhythm generator likely resides in the eyestalks (Strauss & Dircksen 2010). However, knowledge on the interaction of both tissues on transcriptional level is scarce. By comparing both tissues at the same time within the same individuals, the course and the range of relative mRNA levels of *Clk, Cry2, Cwo, E75, Per, Tim* and *Vri* indicated no significant differences (Figure 15a,b,c,f,g,l,j). Only in *Vri,* a trend could be shown that, the last two time points indicated higher relative mRNA levels during night, within the eyestalks (Figure 15j). Based on these results, it can be assumed that both tissues are equally important for the gene expression of the examined genes. For *Cyc*, three of eight investigated time points, and for *Sgg*, two of eight investigated time points, indicated significant higher mRNA levels in the brain and in the eyestalks. Thus, the course of the relative mRNA levels was the same in both tissues and not all investigated time points indicated significant differences between the tissues, it is difficult to make a statement whether gene expression may play a more prominent role in one of the investigated tissues. Interestingly, our results indicated for *Dbt*, accepted for one investigated time point, significantly higher relative mRNA levels in the brain. As a result of the same course of relative mRNA levels in both tissues, it can be assumed that the gene expression of *Dbt* might be more important role in the brain than in the eyestalks. Thus, *Dbt* is the only gene where we could clearly

conclude that for the detection of potential gene expression pattern, the brain is more suitable. In conclusion, due to the quite similar gene expression patterns in both tissues, for future experiments it is better to work with the whole head, to eliminate potential sources of error in tissue separation.

4.1.3 Potential interactions between the tissues

Neurotransmission, a fundamental process happens in a fraction of a second and constitutes an important part of the transmission of information from cell to cell - neurons to their respective targets. This process regulates both, excitatory and inhibitory functions, in the central nervous system (CNS), underlies sensory processing and regulates autonomic motion (Raven et al. 1996). Within this complex process, the use of electrical potential and chemical signaling agents are involved. Neurons are the basic information processing structures in the CNS. In the fruit fly, this process and involved interactions are already well established. Circadian clocks, the pathway by which the pacemakers neurons transfer the circadian information's to the subsequent cells are involved within the neuronal network (Helfrich-Forster 1995). Rhythmic cycles of clock gene expression as well as subcellular localization were assigned to a set of pacemaker neurons that control circadian rhythms of locomotor activity in *Drosophila* (Blanchardon et al. 2001; Kaneko et al. 2000; Renn et al. 1999). Light inputs via neuronal signals, originating in the eyes, activate pacemaker cells and entrain behavioural rhythms (Helfrich-Förster et al. 2001; Emery et al. 1998). In crustaceans, neuroanatomy as well as their association with identified chemical mediators is much less studied and only roughly located at tissue level (Strauss & Dircksen 2010). To date, the general mechanism how signals are induced, the interactions between the tissues and the signaling of the individual genes is unknown. Interestingly, the comparison of the relative mRNA maxima in the respective tissues over time often indicated a defined temporal shift between the genes examined. In the brain, for *Cry2, E75* and *Per* we determined highest relative mRNA levels at ZT4 and ZT16 (Figure 16). Interestingly, *Clk, Cwo, Cyc, Dbt*, and *Sgg* maximum mRNA expression was shifted by 4 hours, in relation to ZT4 and ZT16 where *Cry2, E75* and *Per* indicated highest relative mRNA levels (Figure 16). In the eyestalks the same pattern could be shown, but less pronounced. These temporally defined shifts in maximum mRNA expression between genes may indicate that signal transduction took place between the genes and may even be induced by the same stimuli. Considering the maxima of the relative mRNA levels of a particular gene between brain and eyestalks, findings indicated even between tissues a time shift. However, these shifts often demonstrated longer time intervals up to 12 hours, which may be an indication that the signal transmission between the tissues is significantly slower or the

signaling of the pacemaker is different between the tissues than within a tissue. Therefore, a variety of questions need to be answered in the future in order to understand the interactions of clock genes: How do the distinct pacemakers connect, synchronise and entrain, within and between tissues? Where are the synaptic connections?

4.1.4 Improvements and important clues for future studies

When studying gene expression of biologically distinct individuals, methodological limitations occur: i) differences in gene expression levels due to biological variation. For example, for the optimization of housekeepers for expression analysis, biological replicates had to be removed due to outlier identification (see 2.8.1 Data quality control) and ii) sex specific differences. Here the sex of the animals was not taken into account and therefore, different patterns of gene expression affected by different sex can not be excluded.

Additionally, improvements of the experimental design should be taken into account. During the experiment no feeding took place (usually the feeding took place every morning), animals caught later during experiment were in a different condition/feeding cue was missing. Therefore, an influence due to the lack of feeding can not be excluded. This is especially true, as a close link between metabolic activity and clock gene expression was already shown in krill by (Teschke et al. 2011).

Another target of this study was to determine if there are differences gene expression levels between the two tissues examined, in order to find the optimal tissue for further investigations in the future. Focusing on brain and eyestalk tissues, as already known as important tissues in crustacean due to containing circadian clocks (Strauss & Dircksen 2010; Yan et al. 2006), in Antarctic krill, it could also be shown that both tissues are suitable for the identification of clock gene expression. However, the tissue-specific investigation of gene expression patterns in brain and eyestalks obtained that the oscillation amplitudes are still very small/not clear as in previous experiments with the whole head. In addition, it could be shown that for only *Dbt,* brain, is the more suitable tissue type for future investigation due to the 2-fold higher expression of this gene. Due to the fact that no difference in the tissues can be recognized for all other genes and the separation is always a potential source of error, it must be considered whether the work-intensive dissection of the head into the individual tissues is meaningful, for the future. Nevertheless, more attention needs to be paid to the exact morphology of the krill head. Little is known about which structures belong to the brain because until now only analyzes with the whole head or with the eyestalks were done (Biscontin et al. 2008; De Pittà et al. 2008; Mazzotta et al. 2010; Teschke et al. 2011; Kilada et al. 2017; Biscontin

et al. 2017). As a result, it cannot be excluded that possibly errors in the separation of the tissues may have been made.

5 Conclusion

Generally, in marine crustaceans and specifically in krill, knowledge about clock genes and their products with respect to oscillatory activity, distribution, and chronobiological functions is scarce.

The methodical part of the present study aimed to optimize gene expression patterns, due to tissue-specific analysis, for future studies. Thus, the tissue specific gene expression showed significant 24h rhythmic oscillation for *Cyc* and *Vri* in brain and eyestalk, as well as more pronounced correlations between the genes within the eyestalks. However, the tissue-specific amplitudes of oscillation are not more pronounced and therefore obtained same results by using the whole head.

However, we were able to show higher gene expression of *Dbt* in the brain, concluding that its gene expression might be more important in this tissue than in the eyestalks. All in all, brain and eyestalks are suitable tissues for the identification of oscillatory rhythms in krill. However, we conclude that the analysis of the whole head is more suitable for the future, because amplitudes of the oscillation are the same and only *Dbt* obtained differences in gene expression within the tissues. Moreover, the dissection of the head entails high sources of error as krill is just too small to cleanly separate the tissues from each other.

The chronological order of the maximum relative mRNA levels, measured in this study, indicated that most genes peaked synchronous or shifted by ~4 hours within the respective tissue. However, because most oscillatory patterns could not clearly be identified, a putative co-regulation of the individual genes can only be cautiously assumed. Furthermore, it could be shown that most of the maximum gene expression levels are often synchronized in both tissues of shifted by ~12 hours. In crustaceans, neuroanatomy research is still in the early stages. However, to contribute to the overall understanding of clock genes and their functions, this important field should be more recognized in future chronobiologic research. Therefore, future studies need to focus the entrainment of distinct pacemakers as well as on the synchronization of individual components of the clock within and between tissues, thereby identifying possible signal transmission pipelines in the krill head.

Recapitulating, this study identified significant 24h oscillatory rhythms in the mRNA expression of two important clock genes brain and eyestalks in krill and in general more pronounced patterns and agreement with literature, within the eyestalks. We further

conclude that gene expression probably play the same role in both tissues, except for *Dbt*, and found initial evidence that the interactions between the genes within a tissue might be displaced by a 4 hour rhythm as well as that the transmission between the tissues needs a larger time frame.

6 Outlook

Mus musculus and *Drosophila*, model organisms which have been extensively studied over a long period of time already provide a lot of knowledge on chronobiological behavior and the associated endogenous timing system, on the contributions of individual clock genes on transcriptional as well as on protein level as well as on neuroanatomical signal perception and transmission (Hardin 2005; Williams & Sehgal 2001; Sokolowski 2001; Dunlap 1999; Herzog et al. 1998; Herzog 2007). In Antarctic krill (*E. superba*), a polar marine non-model organism, only a fraction of this system could yet be investigated. However, with the identification of the *E. superba* transcriptome in 2017 (Hunt et al. 2017), a first molecular framework was provided.

As a first step, detailed studies are needed in the future in order to characterize the clock system in krill. Individual clock genes need to be studied in relation to possible trigger mechanisms (*Zeitgeber*) on mRNA as well as on protein level to determine a functional relationship within the krill endogenous clock system. However, in order to clearly define the regulatory network as well as the functional relationships of clock genes, a knock-out of the respective gene must be implemented. For example, in biomedical research knock-out mice have already been used over decades in order to investigate the effects (metabolic deficits, cardiovascular problems, immune dysfunction, difficulty sleeping and cognitive deficits) of the disruption of the circadian system (Colwell 2015; Yu & Weaver 2011). Also for *Drosophila* knock-out cell lines do already exist, however, however this methodological aspect in krill does not seem to be possible. Problems such as the difficult keeping of krill in captivity, focused reproduction as well as molecular genetic work on this small organism will be a huge challenge to science in the future.

In addition, the exact localization of clock components should be determined. As already shown in *Drosophila*, anti-PER-labeled neurons are located between the inner margin of the medulla neuropil and the central brain, and the expression of PER within these neurons, could be identified to be important for the generation of circadian locomotor activity (Frisch et al. 1996; Siwicki et al. 1988; Zerr et al. 1990; Dushay et al. 1989). To assess, responsibilities and interactions, synchronization and entrainment of the clock genes within and between tissues, the cellular distribution had to be defined.

This approach is currently limited by the availability of krill specific antibodies. However, in the marine zebrafish, anti-mouse CLK antibodies could be used, therefore it would probably be worthwhile to test already existing antibodies from the fruit fly for the suitability in krill (Lahiri et al. 2005).

We can see that much work needs to be done in the future on the circadian clock system in Antarctic krill in order to completely understand how important ecological and physiological processes as e.g. metabolic activity etc. are regulated by this endogenous timing system. However, the data collected in this thesis can be used for a first overview if there are parallel, within the same krill population, between respiratory and DVM results caused by the endogenous timing system. An interesting aspect in future studies is the comparison, of the mentioned experimental setup, with data (same experimental setup) from animals in the field, to investigate how krill is affected in captivity on the basis of its circadian timing.

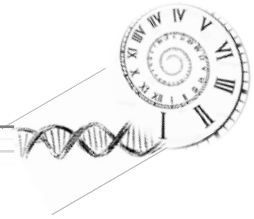

7 Acknowledgement

I would like to express my gratitude to my first supervisor Prof. Dr. Bettina Meyer for the opportunity to be part of her working group and part of such a complex and impressive project. I had the opportunity to see the animals at first hand and to take the samples for my masterthesis by myself. In particular, I would like to thank Fabio Piccolin for his expertise and valuable help, his support and patience and, not least for having always fun at work. I am grateful to the very valuable comments of Katharina Michael on this thesis. I would also like to acknowledge Stefanie Moorthi for being so spontaneous my co-supervisor. I would also like to thank Alberto Biscontin for his preparation of the spikes and for his patient help and to answer our questions with regard to the development of the spikes. A big thank you goes to the whole working group for the enjoyable working atmosphere which made the time at the AWI wonderful.

Apart from the scientific help from each of the working group, I would like to express my great gratitude to my family and Dominik for the help on all conceivable ways.

8 Appendix

Table 4: Results of statistical RAIN analysis in brain implemented by R. The data were adjusted in a 24h period to a sinusoidal curve. P-values and the phases of the sinusoidal curve (amplitude of the oscillation is maximal) are shown in the table for each gene. Significant values are indicated in bold. Significant p-values were then corrected for multiple comparison using the fdr method of Benjamini, Hochberg, and Yekutieli

gene	p-value	phase	fdr-adjustment
Clk	0.757	24	
Cyc	**0.029**	**24**	**0.029**
Per	0.870	24	
Tim	0.837	24	
Cry2	0.838	24	
Cwo	0.052	24	
Vri	**0.017**	**4**	**0.029**
E75	0.394	24	
Sgg	0.644	24	
Dbt	0.821	24	

Table 5: Results of statistical RAIN analysis in eyestalk implemented by R. The data were adjusted in a 24h period to a sinusoidal curve. P-values and the phases of the sinusoidal curve (amplitude of the oscillation is maximal) are shown in the table for each gene. Significant values are indicated in bold. Significant p-values were then corrected for multiple comparison using the fdr method of Benjamini, Hochberg, and Yekutieli

gene	p-value	phase	fdr-adjustment
Clk	0.942	24	
Cyc	**0.018**	24	**0.029**
Per	0.062	24	
Tim	0.789	24	
Cry2	0.849	24	
Cwo	0.176	24	
Vri	**0.026**	4	**0.029**
E75	0.875	24	
Sgg	0.901	4	
Dbt	0.322	20	

Table 6: Significant p-values in eyestalks of Kruskal–Wallis non-parametric ANOVAs followed by multiple t-tests corrected for multiple comparisons (Bonferroni method). Comparison of differences between time points within a gene.

	Kruskal-Wallis	adjustment:bonferroni	
Dbt	0.008163	TP1-TP7	0.042
Per	0.00593	TP2-TP6	0.0083
		TP2-TP7	0.0289
Vri	0.002036	TP7-TP2	0.024
		TP7-TP5	0.019

Table 7: P-values of Mann-Whitney-Wilcoxon test. To compare the level of gene expression for each time point (TP) between eyestalk and brain tissues the Mann-Whitney-Wilcoxon test were used and significant results marked with bold letters

	Clf_F	*Cyc*	*Per*	*Tim_F*	*Cry2*	*Cwo*	*Vri*	*E75*	*Sgg*	*Dbt*
TP1	0.8665	0.1206	0.6126	0.3969	0.3969	0.2319	0.5358	0.6943	0.6126	**0.00124**
TP2	0.3176	**0.02622**	0.2593	0.4557	0.62	0.535	0.9015	0.2593	0.1282	**0.01107**
TP3	0.3939	0.5887	0.9372	0.6991	0.8182	0.06494	0.3939	0.4848	0.06494	**0.00217**
TP4	0.8785	**0.01476**	0.7209	0.6454	0.8785	0.3282	0.9591	0.5054	0.2786	**0.00109**
TP5	0.6126	0.1893	0.6943	0.1893	0.07211	0.05408	0.6943	0.6126	0.4634	0.2319
TP6	0.8148	**0.01111**	0.743	0.5414	0.5414	0.3213	0.8148	0.743	0.3704	**0.00790**
TP7	0.673	0.4234	0.4807	0.673	0.1996	0.2359	0.1388	0.05923	**0.01111**	**0.01111**
TP8	0.4807	0.2766	0.6058	0.2766	0.5414	0.1139	0.0464	0.4234	**0.00247**	**0.0274**

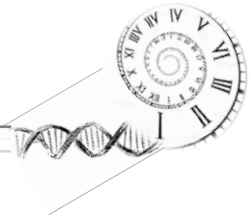

References

Amrein, H. & Bray, S., 2003. Circadian Clocks : A Tale of Two Feedback Loops. *Cell*, pp.284–286.

Andersen, C.L. et al., 2004. Normalization of Real-Time quantitative reverse transcription- PCR data: a model-based variance estimation approach to identify genes suited for normalization, applied to bladder and colon cancer data sets. *Cancer Research*, 64, pp.5245–5250. Available at: http://dx.doi.org/10.1158/0008-5472.CAN-04-0496.

Aréchiga, H. et al., 1993. The circadian system of crustaceans. *Chronobiology international*, 10(1), pp.1–19.

Arechiga, H. & Rodriguez-Sosa, L., 1998. Circadian clock function in isolated eyestalk tissue of crayfish. *Proceedings of the Royal Society B: Biological Sciences*, 265(1408), pp.1819–1823. Available at: http://www.pubmedcentral.nih.gov/articlerender.fcgi?artid=1689369&tool=pmcentrez&rendertype=abstract%5Cnhttp://rspb.royalsocietypublishing.org/cgi/doi/10.1098/rspb.1998.0507.

Aréchiga, H. & Rodríguez-Sosa, L., 2002. Distributed Circadian Rhythmicity In The Crustacean Nervous System. In *The Crustacean Nervous System*. Berlin, Heidelberg: Springer Berlin Heidelberg, pp. 113–122. Available at: http://link.springer.com/10.1007/978-3-662-04843-6_8 [Accessed October 19, 2017].

Aschoff, J., 1960. Exogenous and Endogenous Components in Circadian Rhythms. *Cold Spring Harbor Symposia on Quantitative Biology*, 25(0), pp.11–28. Available at: http://symposium.cshlp.org/cgi/doi/10.1101/SQB.1960.025.01.004 [Accessed October 13, 2017].

Asoc, 2010. *Antarctic Krill Fisheries and Rapid Ecosystem Change: The Need for Adaptive Management*,

Atkinson, A. et al., 2004. Long-term decline in krill stock and increase in salps within the Southern Ocean. *Nature*, 432(November), pp.100–103.

Atkinson, A. et al., 2008. Oceanic circumpolar habitats of Antarctic krill. *Marine Ecology Progress Series*, 362, pp.1–23.

Benjamini, Y. & Hochberg, Y., 1995. Controlling the False Discovery Rate: a Practical and Powerful Approach to Multiple Testing. *Journal of the Royal Statistical Society. Series B (Methodological)*, 57(1), pp.289–300.

Benjamini, Y. & Yekutieli, D., 2001. The control of the false discovery rate in multiple testing under dependency. *The Annals of Statistics*, 29(4), pp.1165–1188.

Biscontin, A. et al., 2017. Functional characterization of the circadian clock in the Antarctic krill, Euphausia superba. *Scientific Reports*, 7(1), p.17742. Available at: http://www.nature.com/articles/s41598-017-18009-2.

Biscontin, A. et al., 2008. Functional characterization of the circadian clock in the Antarctic krill, Euphausia superba. *Scientific Reports*, 7(1), p.17742.

Blanchardon, E. et al., 2001. Defining the role of Drosophila lateral neurons in the control of circadian rhythms in motor activity and eclosion by targeted genetic ablation and PERIOD protein overexpression. *Eur. J. Neurosci*, 13, pp.871–888.

Blau, J. & Young, M.W., 1999. Cycling vrille expression is required for a functional Drosophila clock. *Cell*, 99(6), pp.661–671.

Breedlove, S.M., 2000. Drosophila cryptochromes: A unique circadian- rhythm photoreceptor. *Nature*, 404(March), pp.456–457.

Brown, M. et al., 2011. Flexible adaptation of the seasonal krill maturity cycle in the laboratorytle. *Plankton research*, 33(5): 821.

Cisewski, B. et al., 2010. Seasonal variation of diel vertical migration of zooplankton from ADCP backscatter time series data in the Lazarev Sea, Antarctica. *Deep-Sea Research Part I: Oceanographic Research Papers*, 57(1), pp.78–94.

Clarke, A. & Harris, C.M., 2003. Polar marine ecosystems: major threats and future change. *Environmental Conservation*, 30(1), pp.1–25.

Colwell, C.S., 2015. *Circadian medicine*, Wiley & Sons, Inc. Available at: https://books.google.de/books?id=fqUbCQAAQBAJ&pg=PA110&lpg=PA110&dq=mice+clock+gene+medicine&source=bl&ots=88KpJnB2wq&sig=FICal1OpSOpBKzp0nwpalTg0nas&hl=de&sa=X&ved=0ahUKEwjZpL_Am8HZAhWOJlAKHRIJBqgQ6AEIjgEwCQ#v=onepage&q=mice clock gene medicine&f=false [Accessed February 25, 2018].

Cortés, T., Ortiz-Rivas, B. & Martínez-Torres, D., 2010. Identification and characterization of circadian clock genes in the pea aphid Acyrthosiphon pisum. *Insect Molecular Biology*, 19(SUPPL. 2), pp.123–139.

Curran, M.A.J. et al., 2003. Ice core evidence for Antarctic sea ice decline since the 1950s. *Science (New York, N.Y.)*, 302(5648), pp.1203–1206.

Dunlap, J.C., 1999. Molecular Bases for Circadian Clocks Review. *Cell*, 96, pp.271–290.

Dushay, M.S., Rosbash, M. & Hall, J.C., 1989. The disconnected Visual System Mutations in Drosophila melanogaster Drastically Disrupt Circadian Rhythms. *Journal of Biological Rhythms*, 4(1), pp.1–27. Available at: http://journals.sagepub.com/doi/10.1177/074873048900400101 [Accessed February 21, 2018].

Emery, P. et al., 1998. CRY, a Drosophila clock and light-regulated cryptochrome, is a major contributor to circadian rhythm resetting and photosensitivity. *Cell*, 95, pp.669–679.

Frisch, B. et al., 1996. Staining in the brain of Pachymorpha sexguttata mediated by an antibody against a Drosophila clock-gene product: Labeling of cells with possible importance for the beetle's circadian rhythms. *Cell and Tissue Research*, 286(3), pp.411–429.

Gaten, E. et al., 2008. Is vertical migration in Antarctic krill (Euphausia superba) influenced by an underlying circadian rhythm? *Journal of genetics*, 87(5), pp.473–483.

Gliwicz, M.Z., 1986. Predation and the evolution of vertical migration in zooplankton. *Nature*, 320(6064), pp.746–748. Available at: http://www.nature.com/doifinder/10.1038/320746a0 [Accessed October 12, 2017].

Glossop, N.R.J. et al., 2003. VRILLE Feeds Back to Control Circadian Transcription of< i> Clock</i> in the< i> Drosophila</i> Circadian Oscillator. *Neuron*, 37(2), pp.249–261.

Godlewska M., 1996. Vertical migrations of Krill (Euphausia superba DANA). *Polskie Archiwum Hydrobiologii*, 43(1), pp.9–63.

Hardin, P.E., 2005. Molecular mechanisms of circadian timekeeping in Drosophila. *Current Biology*, 7(4), pp.235–242.

Helfrich-Forster, C., 1995. The period clock gene is expressed in central nervous system neurons which also produce a neuropeptide that reveals the projections of circadian pacemaker cells within the brain of Drosophila melanogaster. *Neurobiology*, 92, pp.612–616. Available at: http://www.pnas.org/content/pnas/92/2/612.full.pdf [Accessed February 24, 2018].

Helfrich-Förster, C. et al., 2001. The circadian clock of fruit flies is blind after elimination of all known photoreceptors. *Neuron*, 30, pp.249–261.

Hellemans, J. et al., 2007. qBase relative quantification framework and software for management and automated analysis of real-time quantitative PCR data. *Genome biology*, 8(2), p.R19. Available at: http://www.pubmedcentral.nih.gov/articlerender.fcgi?artid=1852402&tool=pmcentrez&rendertype=abstract.

Herzog, E.D., 2007. Neurons and networks in daily rhythms. *Nature Reviews Neuroscience*, 8(10), pp.790–802.

Herzog, E.D., Takahashi, J.S. & Block, G.D., 1998. Clock controls circadian period in isolated suprachiasmatic nucleus neurons. *Nature neuroscience*, 1(8), pp.708–713.

Hill, S.L., Phillips, T. & Atkinson, A., 2013. Potential Climate Change Effects on the Habitat of Antarctic Krill in the Weddell Quadrant of the Southern Ocean. *PLoS ONE*, 8(8).

Hirano, Y., Matsuda, T. & Kawaguchi, S., 2003. Breeding antarctic krill in captivity. *Marine and Freshwater Behaviour and Physiology*, 36(4), pp.259–269. Available at: http://www.tandfonline.com/doi/abs/10.1080/10236240310001614448 [Accessed January 4, 2018].

Hunt, B.J. et al., 2017. The Euphausia superba transcriptome database, SuperbaSE: An online, open resource for researchers. *Ecology and Evolution*, 7(16), pp.6060–6077.

Kaneko, M. et al., 2000. Disruption of synaptic transmission or clock-gene-product oscillations in circadian pacemaker cells of Drosophila cause abnormal behavioral rhythms. *J. Neurobiol*, 43, pp.207–233.

Kawaguchi, S. et al., 2013. Risk maps for Antarctic krill under projected Southern Ocean acidification. *Nature Climate Change*, 3(7), pp.1–5. Available at: http://dx.doi.org/10.1038/nclimate1937.

Kawaguchi, S. et al., 2007. The krill maturity cycle: A conceptual model of the seasonal cycle in Antarctic krill. *Polar Biology*, 30(6), pp.689–698.

Kilada, R. et al., 2017. Validation of band counts in eyestalks for the determination of age of Antarctic krill, Euphausia superba. *PLoS ONE*, 12(2), pp.1–14.

King, R., Nicol, S. & KM., C.P.&, 2003. Krill maintenance and experimentation at the Australian Antarctic Division. *Marine and Freshwater Behaviour and Physiology*, 36, pp.271–283.

Kuhlman, S.J., Mackey, S.R. & Duffy, J.F., 2007. Biological rhythms workshop I: Introduction to chronobiology. *Cold Spring Harbor Symposia on Quantitative Biology*, 72, pp.1–6.

Lahiri, K. et al., 2005. Temperature Regulates Transcription in the Zebrafish Circadian Clock D. Stemple, ed. *PLoS Biology*, 3(11), p.e351. Available at: http://dx.plos.org/10.1371/journal.pbio.0030351 [Accessed February 21, 2018].

Lozán, J.L. & Kausch, H., 1998. *Angewandte Statistik für Naturwissenschaftler*, Parey Buchverlag Berlin.

Matsumoto, A. et al., 2007. A functional genomics strategy reveals clockwork orange as a transcriptional regulator in the Drosophila circadian clock A functional genomics strategy reveals clockwork orange as a transcriptional regulator in the Drosophila circadian clock. , pp.1687–1700.

Mauvoisin, D. et al., 2014. Proteomics and circadian rhythms : It ' s all about signaling ! *Proteomics*, 15(0), pp.1–15.

Mazzotta, G.M. et al., 2010. A Cry from the Krill. *Chronobiology International*, 27(3), pp.425–445.

Meyer, B. et al., 2002. Feeding and energy budgets of Antarctic krill Euphausia superba at the onset of winter--I. Furcilia III larvae. *Limnology and Oceanography*, 47(4), pp.943–952. Available at: http://nora.nerc.ac.uk/10203/.

Meyer, B. et al., 2010. Seasonal variation in body composition, metabolic activity, feeding, and growth of adult krill Euphausia superba in the Lazarev Sea. *Marine Ecology Progress Series*, 398(January), pp.1–18.

Miller, D. G. M. & Hampton, I., 1989. Biology and ecology of the Antarctic krill (Euphausia superba Dana): a review. *BIOMASS 9. Scott Polar Research Institute (SCAR/SCOR): Cambridge, UK.*

Murphy, E.J. et al., 2007. Climatically driven fluctuations in Southern Ocean ecosystems. *Proceedings. Biological sciences / The Royal Society*, 274(1629), pp.3057–3067.

Naylor, E. & Emeritus, P., 2010. Chronobiology of Marine Organisms. *Cambridge Univ Press*. Available at: www.cambridge.org [Accessed October 19, 2017].

Nicol, S. & Yoshinari, E., 1997. *Krill fisheries of the world* 367th ed., FAO Fisheries Technical Paper. Available at: https://books.google.de/books?hl=de&lr=&id=V3invKEp5q0C&oi=fnd&pg=PA1&dq=Krill+fisheries&ots=pzNPFQ4TA4&sig=od6jJzpN5Scm9Or6_iGJt5aJbEE#v=onepage&q=Krill fisheries&f=false [Accessed December 11, 2017].

De Pittà, C. et al., 2008. Systematic sequencing of mRNA from the Antarctic krill (Euphausia superba) and first tissue specific transcriptional signature. *BMC Genomics*, 9, pp.1–14.

De Pittà, C. et al., 2013. The Antarctic Krill Euphausia superba Shows Diurnal Cycles of Transcription under Natural Conditions. *PLoS ONE*, 8(7).

Pittendrigh C, 1981. Circadian rhythms and entrainment. *Aschoff J (ed) Handbook of behavioral neurobiology*, 4, p.pp 95–124.

Price, J.L. et al., 1998. Doubletime is a new Drosophila clock gene that regulates PERIOD protein accumulation. *Cell*, 94, pp.83–95.

Quetin, L.B. & Ross, R.M., 1991. Behavioral and Physiological Characteristics of the. *American Zoologist*, 63(December 1988), pp.49–63.

Raven, P.H. et al., 1996. *Opportunities in Biology*, NATIONAL ACADEMY PRESS Washington, D.C. 1989.

Renn, S.. et al., 1999. A pdf neuropeptide gene mutation and ablation of PDF neurons each cause severe abnormalities of behavioral circadian rhythms in Drosophila. *Cell*, 99, pp.791–802.

Roenneberg, T. & Merrow, M., 2005. Circadian clocks - the fall and rise of physiology. *Molecular Cell Biology*, 6(December), pp.965–971. Available at: http://dx.doi.org/10.1038/nrm1766.

Rubin, E.B. et al., 2006. Molecular and phylogenetic analyses reveal mammalian-like clockwork in the honey bee (*Apis mellifera*) and shed new light on the molecular evolution of the circadian clock. *Genome Research*, 16, pp.1352–1365. Available at: http://genome.cshlp.org/content/16/11/1352.short.

Sales, G. et al., 2017. KrillDB: A de novo transcriptome database for the Antarctic krill (Euphausia superba). *PLoS ONE*, 12(2), pp.1–12.

Sandeman, D. et al., 1992. Morphology of the Brain of Crayfish, Crabs, and Spiny Lobsters: A Common Nomenclature for Homologous Structures. *The Biological Bulletin*, 183(2), pp.304–326. Available at: http://www.journals.uchicago.edu/doi/10.2307/1542217 [Accessed October 19, 2017].

Sbragaglia, V. et al., 2015. Identification, characterization, and diel pattern of expression of canonical clock genes in Nephrops norvegicus (crustacea: Decapoda) eyestalk. *PLoS ONE*, 10(11), pp.1–17.

Schiermeier, Q., 2010. Ecologists fear Antarctic krill crisis. *Nature*, 467, p.28.

Siegel, V., 2016. *Biology and ecology of the Antarctic krill* ISSN 2468-. V. Siegel, ed., Springer.

Siegel, V., 2005. Distribution and population dynamics of Euphausia superba: Summary of recent findings. *Polar Biology*, 29(1), pp.1–22.

Siegel, V. et al., 2004. Krill demography and large-scale distribution in the southwest Atlantic during January/February 2000. *Deep-Sea Research Part II: Topical Studies in Oceanography*, 51(12–13 SPEC.ISS.), pp.1253–1273.

Siwicki, K.K. et al., 1988. Antibodies to the period gene product of Drosophila reveal diverse tissue distribution and rhythmic changes in the visual system. *Neuron*, 1(2), pp.141–50. Available at: http://www.ncbi.nlm.nih.gov/pubmed/3152288 [Accessed February 21, 2018].

Sokolowski, M.B., 2001. Drosophila: Genetics Meets Behaviour. *Nature Reviews. Genetics*, 2(11), pp.879–890. Available at: http://libproxy.lib.unc.edu/login?url=https://search.proquest.com/docview/223751727?accountid=14244%0Ahttp://vb3lk7eb4t.search.serialssolutions.com/?genre=article&atitle=DROSOPHILA%3A+GENETICS+MEETS+BEHAVIOUR&author=Sokolowski%2C+Marla+B&volume=2&issue=11.

Strauss, J. & Dircksen, H., 2010. Circadian clocks in crustaceans: identified neuronal and cellular systems. *Front Bioscience*, 15, pp.1040–1074.

Taki, K., Hayashi, T. & Naganobu, M., 2005. Characteristics of seasonal variation in diurnal vertical migration and aggregation of Antarctic krill (Euphausia superba) in the Scotia Sea, using japanese fishery data. *CCAMLR Science*, 12, pp.163–172.

Teschke, M. et al., 2011. A circadian clock in antarctic krill: An endogenous timing system governs metabolic output rhythms in the euphausid species Euphausia superba. *PLoS ONE*, 6(10).

Teschke, M., Kawaguchi, S. & Meyer, B., 2008. Effects of simulated light regimes on maturity and body composition of Antarctic krill , Euphausia superba. , pp.315–324.

Teschke, M., Kawaguchi, S. & Meyer, B., 2007. Simulated light regimes affect feeding and metabolism of Antarctic krill, Euphausia superba. *Limnology and Oceanography*, 52(3), pp.1046–1054. Available at: http://www.jstor.org/stable/4499677.

Thaben, P.F. & Westermark, P.O., 2014. Detecting rhythms in time series with rain. *Journal of Biological Rhythms*, 29(6), pp.391–400.

Thomas, P.G. & Ikeda, T., 1987. Sexual regression, shrinkage, re-matruation and growth of spent female Euphausia superba in the laboratory. *Marine Biology*, 95, pp.357–363.

Tomioka, K. & Matsumoto, A., 2015. Circadian molecular clockworks in non-model insects. *Current Opinion in Insect Science*, 7, pp.58–64. Available at: http://dx.doi.org/10.1016/j.cois.2014.12.006.

Williams, J. a & Sehgal, A., 2001. M Olecular C Omponents of the C Ircadian S Ystem in D Rosophila. *Most*, pp.121–138.

Yan, J.-S. et al., 2006. Molecular cloning of Clock cDNA from the prawn, Macrobrachium rosenbergii. *Brain Research*, 1067(1), pp.13–24. Available at: http://www.sciencedirect.com/science/article/pii/S000689930501382X [Accessed October 19, 2017].

Yu, E.A. & Weaver, D.R., 2011. Disrupting the circadian clock: gene-specific effects on aging, cancer, and other phenotypes. *Aging*, 3(5), pp.479–93. Available at: http://www.ncbi.nlm.nih.gov/pubmed/21566258 [Accessed February 25, 2018].

Zane, L. et al., 1998. Molecular evidence for genetic subdivision of Antarctic krill (Euphausia superba Dana) populations. *Proceedings of the Royal Society of London B. Biological Sciences*, 265(1413), pp.2387–2391.

Zerr, D.M. et al., 1990. Circadian fluctuations of period protein immunoreactivity in the CNS and the visual system of Drosophila. *The Journal of neuroscience : the official journal of the Society for Neuroscience*, 10(8), pp.2749–62. Available at: http://www.ncbi.nlm.nih.gov/pubmed/2117644 [Accessed February 21, 2018].

Zhu, H. et al., 2008. Cryptochromes define a novel circadian clock mechanism in monarch butterflies that may underlie sun compass navigation. *PLoS Biology*, 6(1), pp.0138–0155.

Zhu, H. et al., 2006. The two CRYs of the butterfly. *Current Biology*, 16(7), p.730.

Statutory declaration

I declare that I have developed and written the enclosed master thesis entitled

Daily patterns of clock gene expression in Antarctic krill. Euphausia superba. under a 12h:12h light:dark cycle in the laboratory

entirely by myself and have not used sources or means without declaration in the text. Any thoughts or quotations which were inferred from these sources are clearly marked as such. Furthermore I assure that I have followed the general principles of scientific work and publication as defined in the guidelines of good scientific practice of the University of Oldenburg.

Oldenburg, March 7. 2018